

Thermal loading studies using the Yucca Mountain unsaturated zone model

Charles B. Haukwa^{*}, Yu-Shu Wu, G.S. Bodvarsson

Earth Sciences Division, Lawrence Berkeley National Laboratory, Berkeley, CA, 94720 USA

Accepted 12 November 1998

Abstract

A systematic modeling study of the effect of thermal loading on moisture, gas, and heat flow in the unsaturated zone of Yucca Mountain has been carried out. The study is based on a two-dimensional (2-D) north–south vertical cross-section, using both the effective continuum and the dual-permeability modeling approaches. A study was also conducted on a three-dimensional (3-D) model using the effective continuum approach. The 2-D model conducted in 1996 uses a average uniform infiltration rate of 4.4 mm/year and a thermal load of 83 kW/acre. The 3-D model uses an spatially varying infiltration rate and a revised average thermal load of 87.6 kW/acre. For the rock properties used in the Topopah Springs (TSw) hydrogeological unit, heat pipe conditions develop above and below the repository in 10–100 years in both models. The average temperature of the boiling zone is about 96°C. This boiling zone is confined to the TSw hydrogeological unit and lasts about 1000 years. At the top of the CHn (vitrific/zeolitic interface), predicted maximum temperature is about 70–75°C after about 2000 years. The model predicts a temperature increase of approximately 30°C at the water table. The results show that thermal loading at the repository also results in significant changes in the moisture distributions at the repository horizon and the zone directly above and below it. A large increase in liquid and gas flux, several orders of magnitude above ambient conditions, is predicted near the repository. This study indicates the ECM and dual-*k* modeling approaches provide similar simulation results, in terms of temperature and moisture flow and distribution. The only difference is that at early times, the ECM model predicts more extensive boiling conditions. Localized dry-out is predicted in areas with low infiltration flux within the central part of the repository. However, because coarse grids were used, average saturation in the matrix blocks representing the repository indicates will remain high even when the regions near repository are completely dry. Analysis of the flux pattern

^{*} Corresponding author. Fax: +1-510-486-6115; e-mail: cbhaukwa@lbl.gov

at the top and bottom boundaries of the repository shows that the liquid always flows into the repository for most the thermal loading period (up to 10,000 years). © 1999 Elsevier Science B.V. All rights reserved.

Keywords: Unsaturated zone thermohydrology; Repository-flux; Effective continuum model (ECM); Dual-permeability (dual- k)

1. Introduction

1.1. Background

The U.S. Department of Energy is performing detailed site characterization studies at Yucca Mountain to determine its suitability as a geological repository site for high level nuclear wastes. As part of these research efforts, a three-dimensional (3-D), site-scale unsaturated zone (UZ) model has been developed at Lawrence Berkeley National Laboratory (LBNL) in collaboration with the U.S. Geological Survey (USGS) (Wittwer et al., 1995; Bodvarsson and Bandurraga, 1996). The continued model development and calibration studies (Ahlers et al., 1995a,b, 1996) have led to a fully coupled 3-D model incorporating known geological and hydrological complexities at Yucca Mountain. The complexities include vertical and lateral geological heterogeneities (Bandurraga, 1996) such as degree of welding and alteration, fault zones and offsets, and varying matrix and fracture properties. The primary objectives of developing the 3-D site-scale model are to predict the ambient hydrogeological conditions and the movement of moisture and gas within the unsaturated zone of the mountain. In addition, the model has the capability of modeling non-isothermal flow and tracer transport phenomena at the mountain. Applications of such a site-scale model include evaluation of the effects of thermo-hydrologic (T-H) and thermal loading processes on moisture, gas, and heat flow through the mountain for long-term performance assessment of the repository.

Heat generated by nuclear waste, emplaced in a partially saturated geological system will significantly redistribute the liquid saturation and flux in the host rock near the repository and thus directly impact the performance of the repository in terms of radionuclide containment. Quantitative evaluation of thermo-hydrologic and thermal loading effects on the performance of the potential high-level nuclear waste repository at Yucca Mountain is essential in conducting site characterization studies to optimize the performance of the natural barrier repository. It will also provide parameters for design of the engineered barrier system (optimal design of waste package containers and associated underground drifts, designed to contain the nuclear waste for periods of 300–1000 years or longer, following permanent closure). After the containment period, the natural barrier system (geological setting and the unsaturated zone) should isolate the waste and maintain acceptable levels of release to the accessible environment for up to 10,000 years. Although laboratory and field studies of thermal loading phenomena have been performed, it is impossible to observe and test thermo-hydrologic conditions over long times and on the scale of the mountain. Numerical modeling will play a crucial role

in understanding the impact of thermal loading on various aspects of the overall waste disposal system. Performance assessment models based on numerical simulation of fluid and heat flow can include all important physical and chemical processes which affect repository and host rock behavior, and explicitly represent relevant thermo–hydrologic conditions at the potential repository site over the length of the project.

1.2. Previous research

Emplacement of heat-generating high-level nuclear wastes at Yucca Mountain would create complex multiphase fluid flow and heat transfer processes. The physical mechanisms include conduction and convection heat transfer, phase change phenomena (boiling and condensation), flow of liquid and gas phases under variably saturated conditions, diffusion and dispersion of vapor and gas, vapor sorption, and vapor pressure lowering effects. The heterogeneity of the complicated geological setting at Yucca Mountain, with alternating layers of variably welded and altered fractured rocks, will significantly affect the processes of fluid and heat flow.

Numerical modeling approaches for simulation of these thermo–hydrologic and thermal loading processes are generally based on geothermal and petroleum reservoir simulation methodology using coupled multiphase fluid and heat flow formulations and finite difference or finite element schemes. A number of numerical repository performance models for evaluating the thermo–hydrologic loading effects of the Yucca Mountain site have been developed by several different groups (e.g., Buscheck et al., 1994; Pruess and Tsang, 1994; Haukwa et al., 1996). Model conceptualizations have focused mainly on large-scale average behavior or on local simplified domains of two-dimensional (2-D) representations. In most cases the effective continuum model (ECM) is used instead of explicit incorporation of fracture effects. This is due to the composition rigor involved in the treatment of matrix–fracture interaction as well as the uncertainties associated with the site characterization of fracture and matrix properties.

Simulation techniques have been used to perform analyses of thermo–hydrologic conditions associated with high-level nuclear wastes since the early 1980's. Mondy et al. (1983) simulated fluid and heat flow using approximate 2-D representations of alternative emplacement geometries with and without ventilation of emplacement drifts. The host rock was modeled as an unfractured porous medium, and no allowance was made for vaporization or vapor transport (two-phase) effects. St. John (1985) presented a thermal analysis for waste package emplacement in vertical boreholes and modeled heat conduction (no fluid flow) in 2-D and 3-D emplacement geometries. The maximum host rock temperature was found to be near 250°C.

Pruess and Wang (1984) reported sensitivity studies on thermo–hydrological conditions near an infinite linear string of waste packages. They modeled fluid and heat flow, including phase change effects in one-dimensional (1-D) cylindrical geometry. They found that strong two-phase vapor–liquid counterflow effects termed ‘heat pipe’ (Ogniewicz and Tien, 1979; Udell, 1985) occurred in some cases. The coupling of T–H response with mechanical deformations of rocks has been investigated in field experiments by Zimmerman and coworkers (Zimmerman, 1983; Zimmerman and Blanford,

model of a 3-km diameter disk-shaped repository to examine the hydrothermal responses. Pruess et al. (1990a,b) performed a comprehensive modeling study of simultaneous transport of heat, liquid water, vapor, and air in partially saturated fractured porous rock, using the TOUGH code (Pruess, 1987). They used a 2-D idealized model and included an explicit consideration of fracture effects. The hydrogeologic parameters they used were representative of the Yucca Mountain nuclear waste repository site. They demonstrated the capability of modeling multiphase, non-isothermal flow of water and air with phase changes in a fractured medium, and obtained certain insights into expected thermo-hydrological conditions near the waste packages.

A series of modeling studies of thermal loading impacts on thermo-hydrologic performance at Yucca Mountain have been performed by a group of researchers at the Lawrence Livermore National Laboratory (LLNL) in recent years. They used the V-TOUGH code (Nitao, 1989) and the effective continuum approximation for treating fracture and matrix interactions. Many simulations and sensitivity studies have been conducted at LLNL in order to evaluate and predict the thermo-hydrologic conditions at the repository (Nitao, 1988; Ramspott, 1991; Buscheck and Nitao, 1991; Nitao et al., 1992; Buscheck and Nitao, 1992, 1993a,b,c,d,e, 1994; Buscheck et al., 1994).

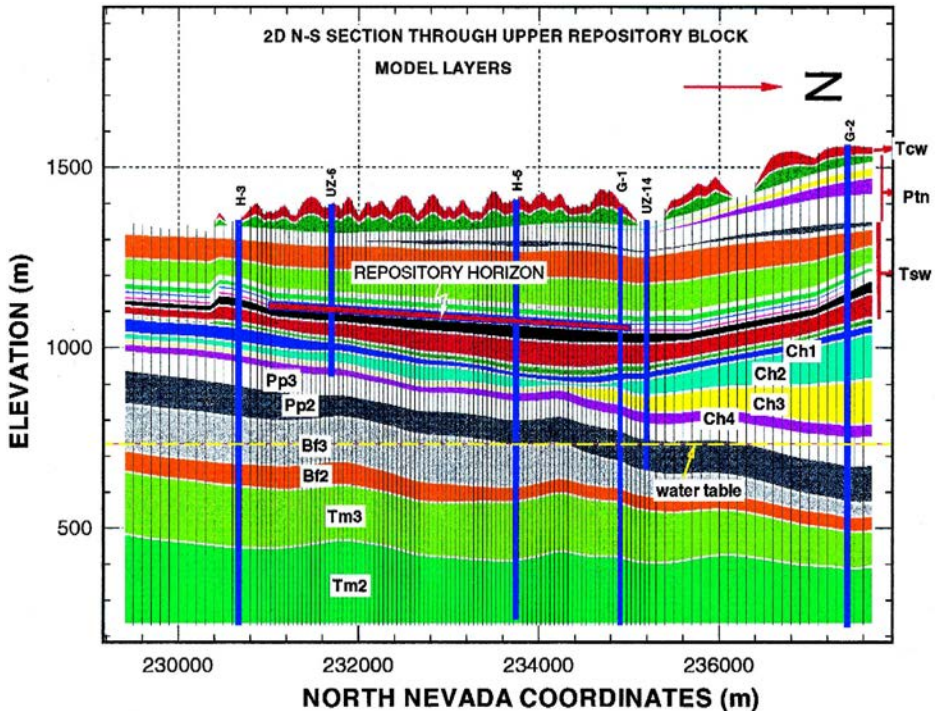


Fig. 2. Dimensional unsaturated zone north-south cross-section A-A', showing model grid layers and hydrogeological units used.

Table 1

The relationship between the geological, hydrogeological units, formation and model grid layers used in the numerical models

Geological unit	Model Grid Layer Name	Hydrogeological unit
PAINTBRUSH GROUP		
Tiva Canyon Tuff	tcw11 tcw12	Tiva Canyon (TCw)
	tcw13	
	ptn21	
Bedded tuff		Paintbrush (PTn)
Yucca Mountain Tuff	ptn22	
Bedded tuff	ptn23	
Pah Canyon Tuff	ptn24	
Bedded tuff		
TOPOPAH SPRING TUFF		
	ptn25	Topopah Spring (TSw)
	tsw31	
	tsw32	
	tsw33	
	tsw34	
	tsw35	
	tsw36	
	tsw37	
CALICO HILLS GROUP		
Bedded tuff	ch1zc, ch1vc	Calico Hills (CHn)
Calico Hills Formation	ch2vc	
	ch3zc	
	ch4zc, ch4vc	
CRATER FLAT GROUP		
Prow Pass Tuff	pp3vp	
	pp2zp	
Bedded tuff		
Upper Bullfrog Tuff		
Middle Bullfrog Tuff	bf3vb	
Lower Bullfrog Tuff	bf2zb	Crater flat Undifferentiated
Upper Tram Tuff	tm3vt	

Table 2

Fracture properties—fracture porosity, aperture and spacing data used for the dual-permeability simulations

Unit	Porosity	Aperture (m)	Spacing (m)
Tcw	1.38e-3	0.181e-3	0.618
Ptn	4.12e-3	0.206e-3	2.220
Tsw	2.75e-3	0.180e-3	0.740
CHn	9.98e-4	0.179e-3	1.618

Some recently developed models (Pruess and Tsang, 1993, 1994) have provided more detailed investigations into strongly heat-driven flow processes at small scales to look at heterogeneity effects. They concluded through these studies that for a highly heterogeneous fractured-porous hydrogeologic system at Yucca Mountain, water infiltration across the unsaturated zone may be dominated by highly localized phenomena, including ‘fast’ channelized flow along preferential paths in fractures, and frequent local ponding. Current performance assessment models focus on volume-averaged behavior with relatively large model grid-blocks, and may not be able to represent such effects.

Mountain-scale T–H modeling studies of Yucca Mountain have also been reported using the following: 2-D cross-sections and the ECM model (Wu et al., 1995); 2-D

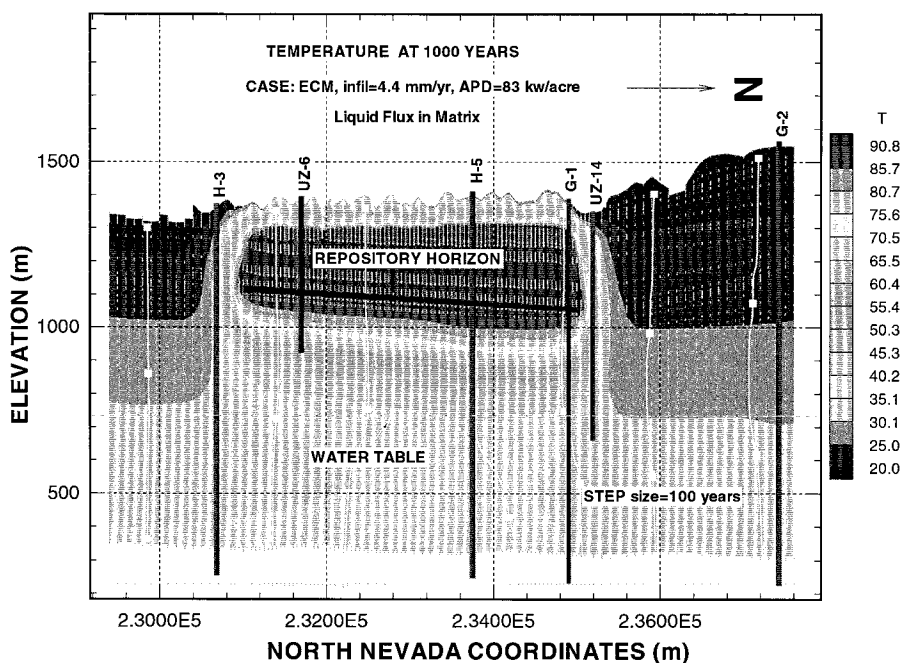


Fig. 3. Temperature distribution after 1000 years thermal loading. Effective Continuum Method; APD = 83 kW/acre, infiltration = 4.4 mm/year. Vectors and flow paths show gas flux matrix continuum.

cross-sections and the dual-permeability model (Haukwa et al., 1996); and 3-D grids and the ECM models (Francis et al., 1996). However, those studies and conclusions need to be further investigated, since the rock properties, conceptual models, and surface infiltration conditions at the site have been updated (Bodvarsson and Bandurraga, 1996). In addition, the 3-D simulations of Francis et al. (1996) were based on a smaller model domain that did not evaluate many effects such as faults on the mountain T–H behavior. To date no 3-D dual-permeability mountain scale thermal loading studies have been performed.

1.3. Objectives and contents

The objectives of this report are to (a) develop both a 2-D and a 3-D mountain-scale T–H model, based on the current 3-D site-scale UZ flow model (Bodvarsson and Bandurraga, 1996); and (b) use the 2-D and 3-D T–H models (that utilize alternative conceptual models) to evaluate the effects of repository thermal loading on fluid flow, heat flow, and on the overall mountain T–H conditions. The 2-D site-scale UZ model provides fundamental insights into several aspects of thermal loading and forms a basis for formulation of 3-D thermal loading studies.

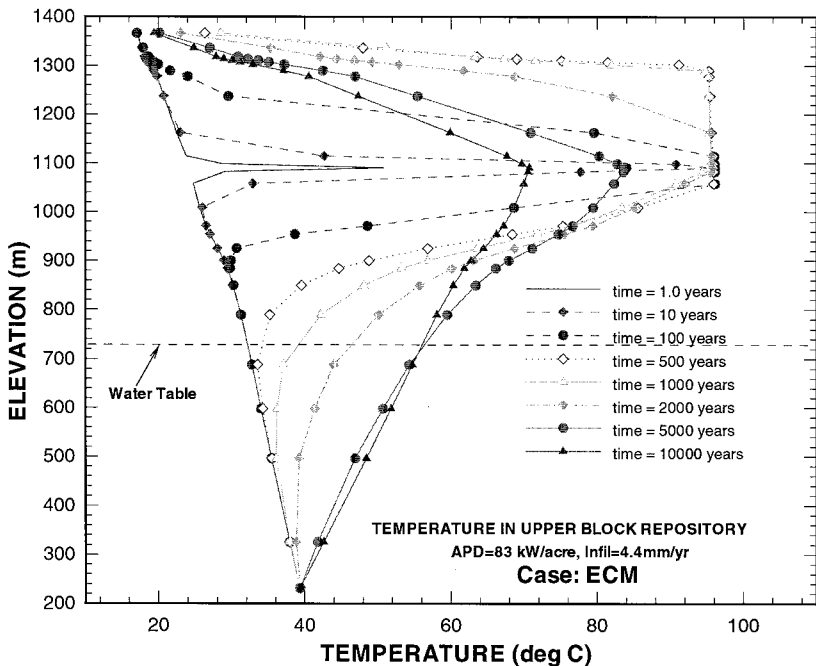


Fig. 4. Vertical temperature profiles through the center of the upper repository block during thermal loading; Effective Continuum Method, APD = 83 kW/acre, infiltration = 4.4 mm/year.

The main efforts involved in the thermal loading studies using the UZ flow model for this paper are as follows

- Describe the UZ flow model, 2-D and 3-D thermal and flow boundary conditions using the Effective Continuum Method (ECM) and Dual-permeability (dual- k) modeling approaches.
- Summarize the model parameters and input data used in the simulations.
- Discuss the modeling results in terms of redistribution of moisture, gas and heat, and the moisture and gas flux through the mountain.
- Evaluate the adequacy of the unsaturated zone model and the (ECM) and (dual- k) modeling schemes in prediction of the evolution of thermohydrologic conditions within the unsaturated zone.
- Investigate the need for using a combined saturated-unsaturated zone model in simulating the Unsaturated Zone thermal response.

1.4. Importance of the thermal loading studies

Quantitative evaluation of the thermohydrologic effects of thermal loading on the performance of the potential nuclear waste repository at Yucca Mountain is essential for

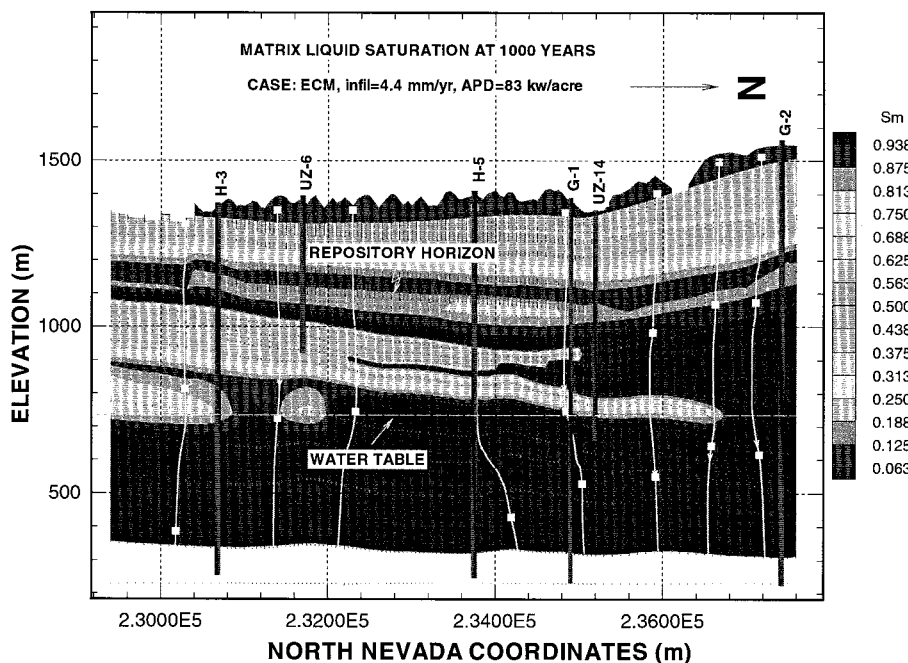


Fig. 5. Matrix continuum liquid saturation after 1000 years thermal loading Effective Continuum Method, APD = 83 kW/acre, infiltration = 4.4 mm/year; Effective Continuum Method, APD 83 kW/acre, infiltration = 4.4 mm/year.

characterization of the behavior of the unsaturated zone and site performance studies, as well as for adequate design of the engineered barrier at the repository. Thermally induced temperature rise, boiling and condensation can lead to mineralogical changes in the unsaturated zone, as well as changes in permeability and porosity due to dissolution and precipitation of solids. These changes could have physical and chemical consequences that could impact the waste isolation (TRW, 1996). Studies of the geology and geochemistry of Yucca Mountain tuffs has established ‘thermal goals’ (temperature limits) for the rock units within and below the potential repository (TRW, 1996). One of the temperature limits sets a maximum of 115°C for the interface of the Topopah Springs (TSw) tuff and the underlying Calico Hills (CHn) non-welded units. This temperature limit is intended to address the concerns that mineralogical changes would occur due to dehydration or re-crystallization induced by repository heating. More recent studies indicate a thermal limit of 90–100°C for the zeolitic Calico Hills units, which are estimated to be about 100 m below the potential repository horizon (TRW, 1996). Another limit sets a maximum of 200°C at 1-m distance from the repository drift wall, because silica phase inversion and temperature gradients can adversely affect the thermal mechanical stability of the repository walls. The thermal cladding limit of 350°C was set to address the potential for canister deterioration under thermal loading due to a combination of stress, corrosion and fatigue. Both the repository drift and the waste canisters are on a much smaller spatial scale than that addressed by the UZ site-scale

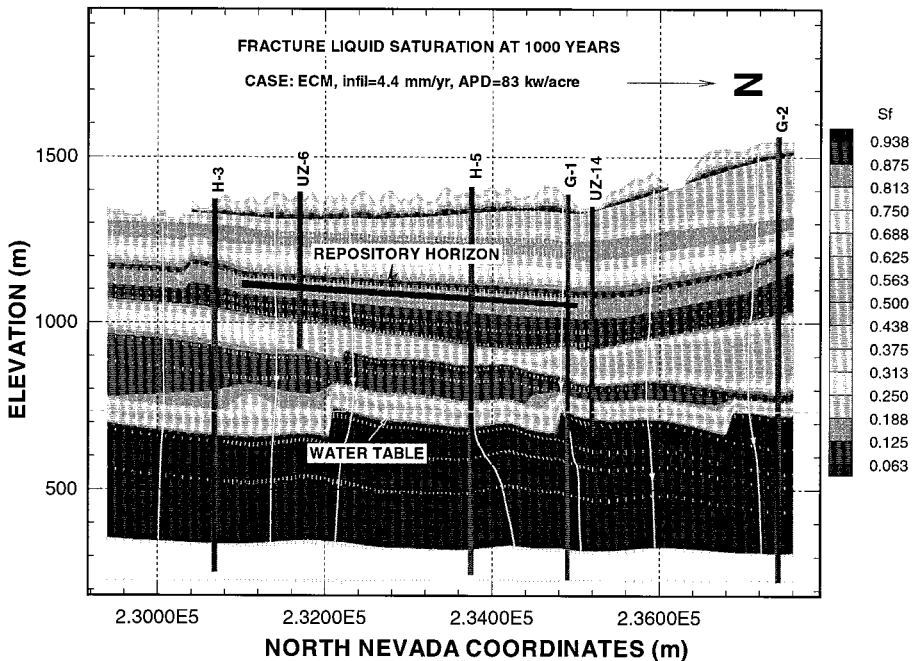


Fig. 6. Fracture continuum liquid saturation after 1000 years thermal loading effective continuum method, APD = 83 kW/acre, infiltration = 4.4 mm/year; Vectors show liquid flux in fractures.

unsaturated zone model which is intended to provide mountain-scale response to thermal loading. Therefore, the site scale model will only be used to investigate the potential for violation of only the first thermal limit, i.e., 90–100°C within the top Calico Hills zeolitic layers. The thermal–hydrologic–chemical (T–H–C) study addresses the potential for heat induced chemical changes in the Mountain (see Sonnenthal et al., this issue).

One consequence of thermal loading is the modification of the ambient flux above and below the repository. Because radionuclide transport occurs primarily through the liquid phase (in the fractures), it is important to quantify the liquid flow at the repository horizon, particularly in the cool down phase of the thermal loading cycle, the period when the integrity of the canisters is impaired by corrosion. Estimation of the period during which the repository remains ‘dry’, and quantification of the liquid flux during the thermal loading cycle, is essential to prediction of the potential for radio-nuclide transport into the saturated zone under various thermal loading scenarios.

In this paper we examine the effects of thermal loading at the repository horizon using a 2-D vertical North–South cross-section model at the center of the upper repository and a 3-D Mountain scale model. The 2-D cross-section model extends from the top of the Tiva (ground surface minus the thickness of the Alluvium), to about 500 m below the water table. This north–south vertical cross-section through the upper repository block was chosen primarily because it crosses the longest extent of the repository. This section also allows us to investigate the influence of the North–South

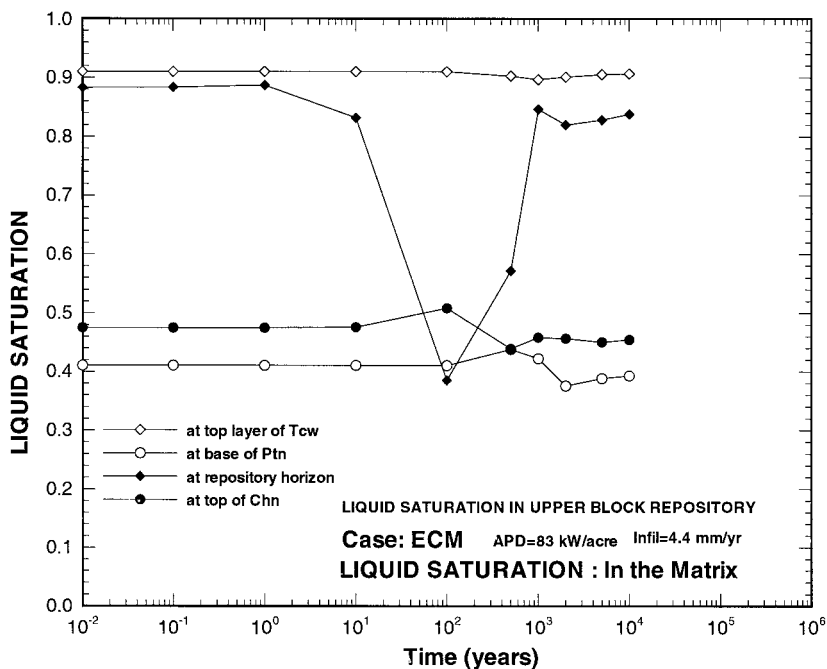


Fig. 7. Liquid saturation at various depths in the center of the upper repository block during thermal loading; Effective Continuum Method, APD = 83 kW/acre, infiltration = 4.4 mm/year.

hydrogeologic layering and the vitric–zeolitic interface in the Calico Hills. The 3-D model uses the same boundary conditions but a spatially variable infiltration rate. Using these models we investigate fluid and heat transfer in the unsaturated zone, and the long-term response of the unsaturated zone and saturated zone to thermal loading at the repository. The numerical simulations were performed using the two-phase numerical code TOUGH2 (Pruess, 1991).

1.5. Modeling approach

In this study the repository is represented by a 6.0-m thick zone that extends 4 km along the cross-section with an average elevation of 1070 m above sea level (masl). For thermal loading studies we assume that thermal loading at the repository horizon over the emplacement period can be represented by an equivalent uniform thermal load at an Area Power Density (APD) of 83 kW/acre (this base rate has now been updated to about 87.6 kW/acre). At this thermal load, equivalent generic total heat vs. time decay curves (M and O, 1995a,b) was used to provide a time dependent heat generation table. This provides a transient heat source at the repository. Under this thermal loading scenario, we performed numerical simulations using the ECM model and using the dual-*k* model. The simulations were carried out for a maximum time of 100,000 years to investigate both the heating and cool down cycles after waste emplacement.

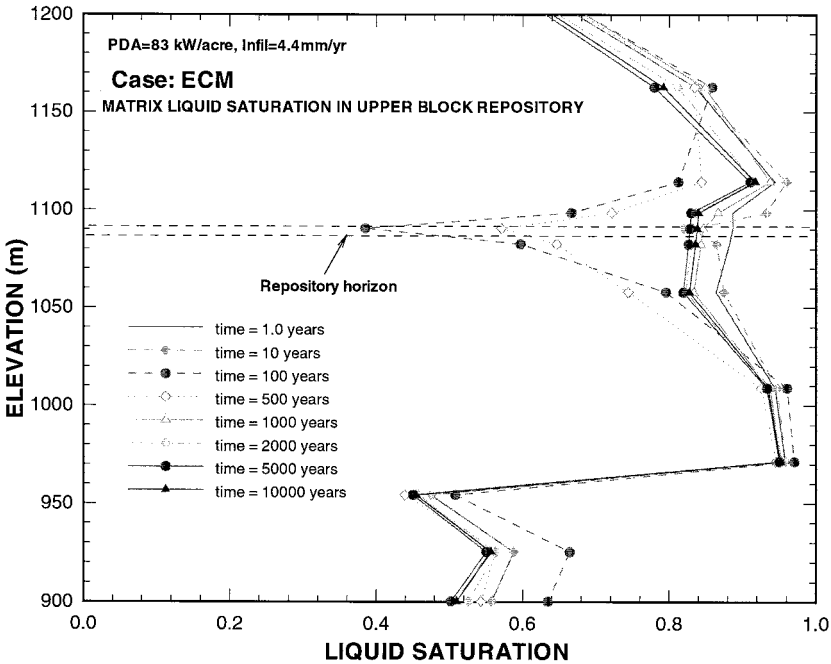


Fig. 8. Vertical saturation profiles through the center of the upper repository block during thermal loading; Effective Continuum Method, APD = 83 kW/acre, infiltration = 4.4 mm/year.

1.5.1. Numerical grids, material properties and boundary conditions for Unsaturated Zone thermal loading studies

Fig. 1 shows a plan view of the 3-dimensional unsaturated zone model and the location of the North–South 2-D vertical cross-section (A–A') used for 2-D thermal hydrological studies. The 2-D vertical cross-section used in this study is refined from the 3-D unsaturated zone site scale model. It has a grid spacing of 50 m over the repository, a spacing of 100 m outside, and a uniform width of 25 m. The thickness of the elements varies from layer to layer with an average 20–50 m near the repository. For thermal studies the 2-D model extends 500 m below the water table into the saturated zone, down to the Calico Hills tram hydrogeological unit. This extension allows for explicit specification of the bottom boundary condition away from the water table in order to examine the effects of thermal loading on the water table (Fig. 2). So at 500 m below the water table $T = \text{constant}$ and $S_1 = 1.0$; at the water table (UZ–SZ interface), $S_1 = 1.0$, $P_g = \text{constant}$ and $T = T(x, y, z, t)$. The same boundary treatment was specified for the 3-D model.

The 6-m thick repository layer is overlaid and underlain by a 10-m thick grid layer. This repository horizon is mainly within the LBNL geological model Topopah Springs stratigraphic sub-layer five (TSw5), (Bandurraga, 1996; Haukwa et al., 1996). The final 2-D model consists of 27 non-uniform grid layers in the four welded and non-welded hydrogeological units and has a total of 3774 grid-blocks and 6438 connections. The

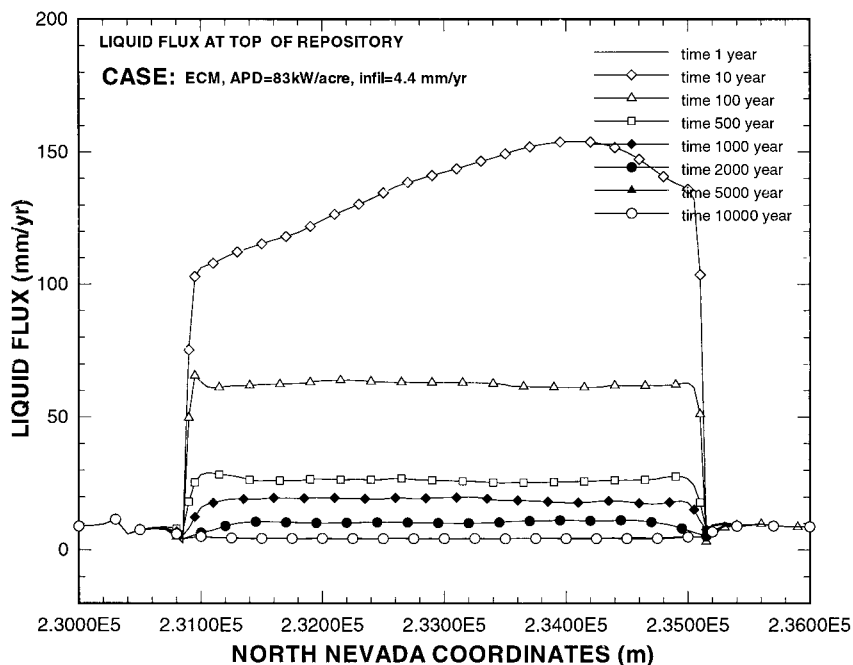


Fig. 9. Liquid flux crossing the top boundary of the Repository; Effective Continuum Method, APD = 83 kW/acre, infiltration 4.4 mm/year.

3-D model has a total of 39,600 elements and 133,400 connections in ECM formulation. It is a relatively coarse model, with a grid spacing 100 m within the repository and 150–300 m outside. Vertically we use the same layer discretization as in the 2-D model.

The material properties of rocks are explicitly allocated based on the elevation of element node, model layer and the hydrogeological unit. The pinch out of Paintbrush unit sub-layers Ptn22 and Ptn24, as well as the zeolitic–vitric interface in the top of the Calico Hills (CHn) units, is explicitly modeled. Rock properties required for numerical simulations in the Tiva Canyon (TCw), Paintbrush (PTn), Topopah springs, and CHn and Prow Pass (Pp) vitric and zeolitic units were (Table 1) obtained from inverse modeling studies using moisture tension and liquid saturation data (Bandurraga, 1996). For the thermal loading studies we use properties obtained for uniform infiltration rate of 4.4 mm/year over the 3-D model area. The properties for the zeolitic Bullfrog (Bf) units as well as the zeolitic Tram (Tm) units (mainly below the water table) were assumed to be the same as for the Prow pass zeolitic units, since there are insufficient data available for independent evaluation of the properties of these units. A similar correspondence of material properties was assumed for the vitric units.

The layer-wise defined transport properties are modeled as fixed parameters in both space and time. It is expected that changes in the transport parameters of both the matrix and fractures may take place due to thermal loading over a period of thousands of years. It is also known that fractured volcanic tuffs may have properties that show strong

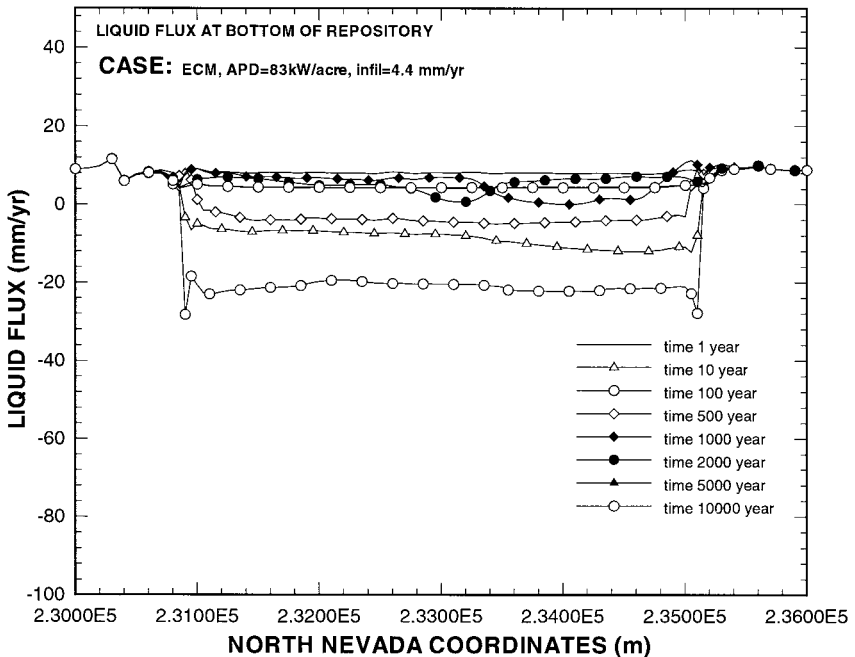


Fig. 10. Liquid flux crossing the bottom boundary of the repository; Effective Continuum Method, APD = 83 kW/acre, infiltration 4.4 mm/year.

variability in their transport properties even within geologically similar units. The study uses a baseline simplified model that neglects, the effects of thermal hydrological chemical and thermal hydrological mechanical coupling as well as flow channeling effects (due heterogeneity in material properties) on the evolution of the flow fields. Future studies can build on such a baseline model by considering the effects of THC or THM coupling. For example, deposition of solids in fractures may drastically change permeability at the repository. Temperature induced stress changes may lead to opening or closing of fractures. Similarly, the distribution of active fractures as well as the variability in transport properties may lead to flow channeling that may be enhanced by thermal loading.

For the thermal studies the following additional thermal properties and model boundary conditions were used. Constant temperature and constant pressure conditions are specified on both top and bottom boundaries. The top boundary temperature was calculated based on surface elevation and observed mean annual temperature. The temperature at the water table was based on the observed temperature distribution from boreholes and the geothermal heat-flow maps (Bodvarsson and Bandurraga, 1996). The spatially-variable bottom boundary temperature, at 500 m below the water table, is based on extrapolation of the water temperature using estimated saturated geothermal gradients of the formations at the water table. This extrapolation results in an increase of about 5°C from the measured values at the water table. The thermal conductivities used in the

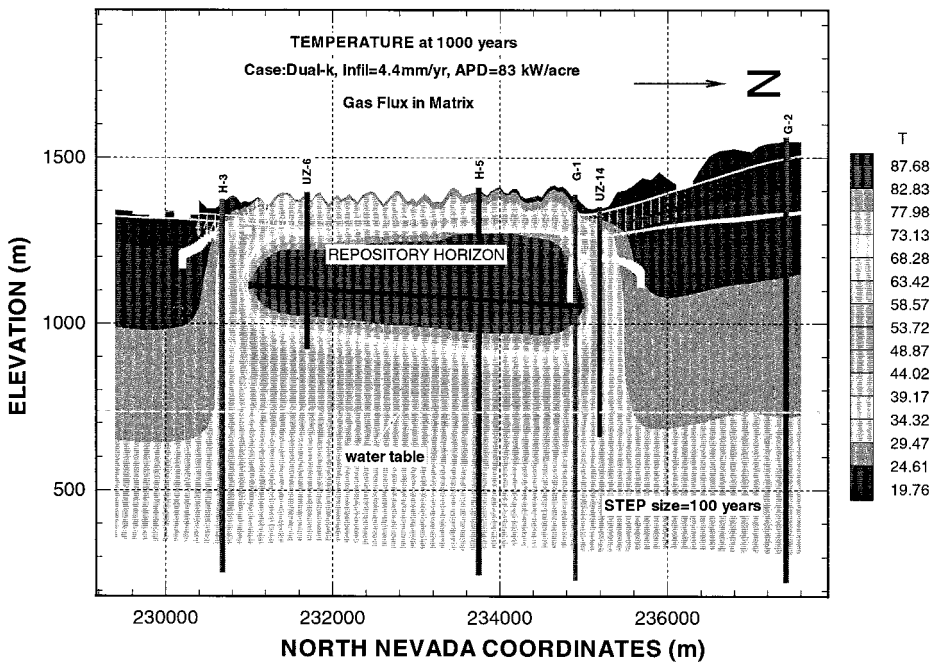


Fig. 11. Temperature distribution after 1000 years thermal loading; Dual-permeability, APD = 83 kW/acre, infiltration = 4.4 mm/year. Vectors and flow paths show liquid flux in matrix continuum.

model are based on estimated saturated and unsaturated thermal conductivity of the UZ hydrogeologic units (Sass et al., 1988; Francis, 1997). Steady state saturated zone conditions were computed assuming a water table at 730 m above sea level (masl), and a hydrostatic pressure gradient below the water table.

1.5.2. Effective continuum method and dual-permeability approaches

The saturated zone and the unsaturated zone at Yucca Mountain consist of different hydrogeologic units that exhibit varying degrees of fracturing. The TCw, TSw and CHn vitric hydrogeologic units contain extensive vertical conductive fractures. The PTn, though very permeable, shows little evidence of fracturing. The zeolitic CHn hydrogeologic units have a low permeability matrix with few fractures. Emplacement of high-level nuclear waste in the unsaturated densely welded and fractured-rock matrix tuffs with highly heterogeneous material properties, will initiate many physical processes due to the thermal load. For example, strong two-phase flow effects in the system will occur. As heat is released from the waste canister and transferred to the surrounding host rock, the temperature near the waste packages will approach or exceed the boiling point of water (approximately 96°C at ambient pressure). Vaporization of formation water will then take place, with associated increases in vapor partial pressure and overall gas phase pressure.

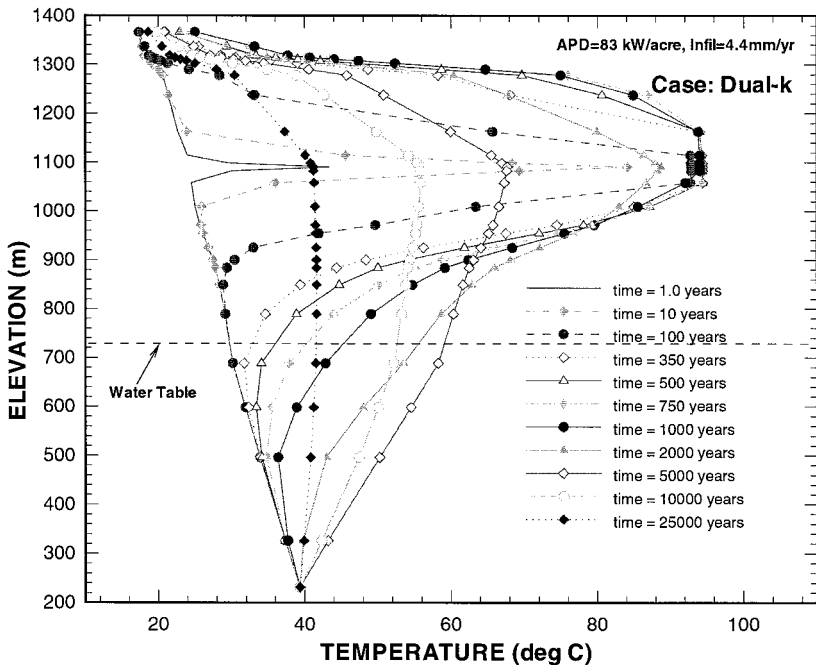


Fig. 12. Vertical temperature profiles through the center of the upper repository block during thermal loading; Dual-permeability, APD = 83 kW/acre, infiltration = 4.4 mm/year.

This vaporization will result in forced convection of the gas phase, with redistribution of the water component accompanied by large latent heat effects. The phase transformation and gas phase flow will perturb the in-situ fluid saturation distribution in both fractures and matrix, thereby setting up capillary pressure gradients and liquid phase flow. These T–H processes associated with thermal loading of the UZ system can be investigated using an ECM formulation or a dual- k formulation for the same 2-D cross-section.

Numerical models of geological systems generally consist of large computational blocks. For example, the 2-dimensional Site Scale model consists of grid blocks with an average dimension of 10–100 m. In the ECM (Wu and Pruess, 1988), these large blocks contain tens to hundreds of fractures that are combined with the matrix to provide an effective continuum with hydraulic properties that mimic the behavior of both the matrix and the fractures. This method of modeling fractured porous media has been used previously in the unsaturated zone flow model (Wittwer et al., 1994; Bodvarsson and Bandurraga, 1996).

In order to effectively capture the physics of the response of a fractured porous medium and to evaluate the effectiveness of the ECM approach, we also developed a dual- k model for the 2-D cross-section model of the Yucca Mountain. The dual-permeability model (Warren and Root, 1963; Pruess and Narasimhan, 1991), allows for explicit

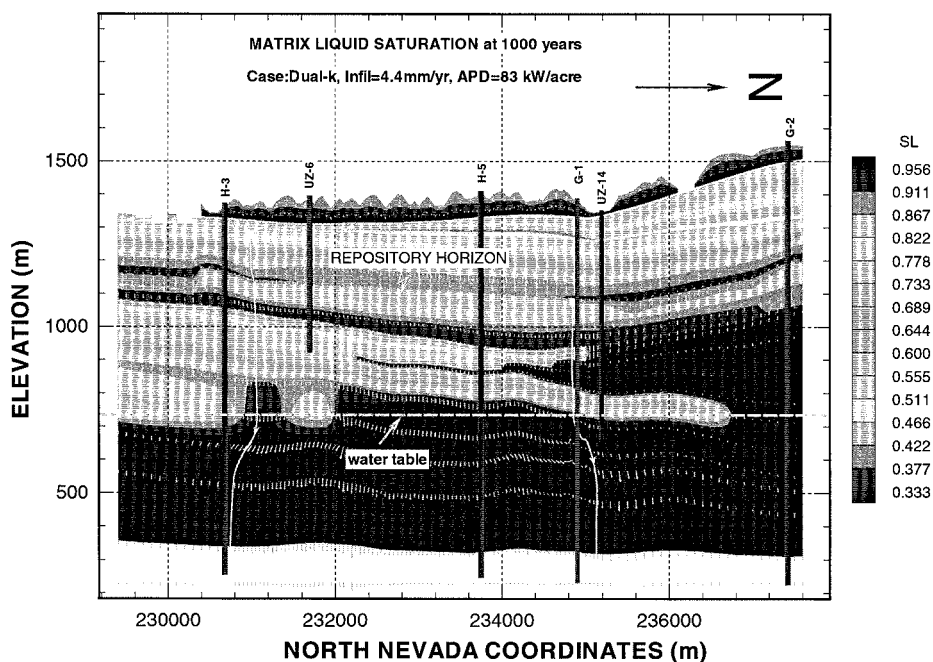


Fig. 13. Matrix continuum liquid saturation after 1000 years thermal loading; Dual-permeability, APD = 83 kW/acre, infiltration = 4.4 mm/year; Dual-permeability, APD 83 kW/acre, infiltration = 4.4 mm/year.

representation of fracture and matrix continua, by separate elements. In our formulation of the dual- k numerical grid, the matrix and fracture are each represented by a single continuum. The fraction of the total volume allocated to fracture elements for each sublayer is equal to twice the fracture porosity of the material in that sublayer. Correct overall fracture porosity is still retained by using a porosity of 0.5 for the fracture continuum porosity. This treatment allows for non-zero fracture heat conductance at zero liquid saturation (i.e., fracture continuum is not entirely fluid filled space). We allow for fracture–fracture, matrix–matrix and fracture–matrix mesh connections and thus global flow occurs in both the fracture and matrix. Because of the large number of nodes in the 3-D model and the large contrast between fracture and matrix continua volumes, no 3-D dual- k thermal loading simulations were performed.

The fracture porosity, aperture and fracture frequencies of the different geological layers used in this 2-dimensional model are based on Table 2. Because they contain very few fractures, the PTn units in the 2-D model were simulated using the single continuum scheme (more recent studies indicate significant fracture transport through the PTn, and future models will consider explicit fracture models in the PTn; and Table 2). This 2-D dual-permeability model was used to simulate thermal loading using a uniform infiltration of 4.4 mm/year (Flint et al., 1996).

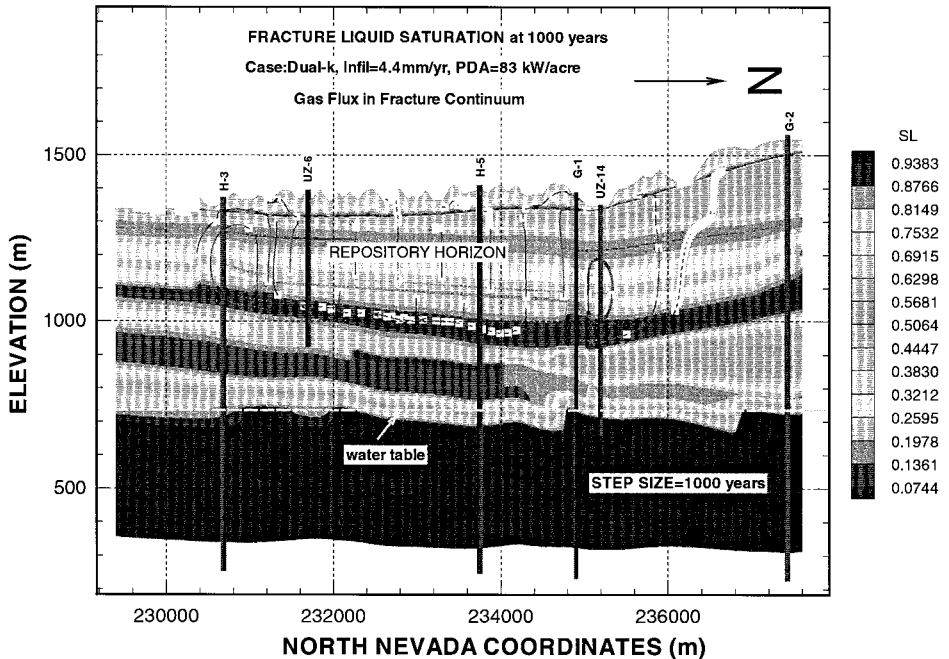


Fig. 14. Fracture continuum liquid saturation after 1000 years thermal loading; Dual-permeability, APD = 83 kW/acre, infiltration = 4.4 mm/year; vectors show liquid flux; Dual-permeability, APD 83 kW/acre, infiltration = 4.4 mm/year. Vectors show gas flux in fractures.

2. Results of numerical simulation

In general, repository heat moves moisture by means of (1) vaporization, (2) driving water vapor from high to low gas-phase pressure zones, (3) condensation, and (4) gravity-capillary driven flow of condensate. The heat transfer and fluid flow are always coupled processes. The physical mechanisms governing heat transfer surrounding a repository include heat conduction and convection (latent and sensible heat flow), and some other minor processes, such as radiation, viscous dissipation and mechanical work, that are usually ignored. Vaporization and condensation of liquid (phase transition) depend on the local temperature, pressure, vapor pressure, and capillarity conditions. The effect of thermal loading on vertical flow of moisture and heat, above and below the repository level can be shown using the 2-D simulation results.

2.1. Effective continuum method simulation results with 4.4 mm/year infiltration, 2-D model

2.1.1. Temperature

The ambient temperature and saturation distribution was simulated using the ECM model with a uniform infiltration rate of 4.4 mm/year. Starting with these ambient

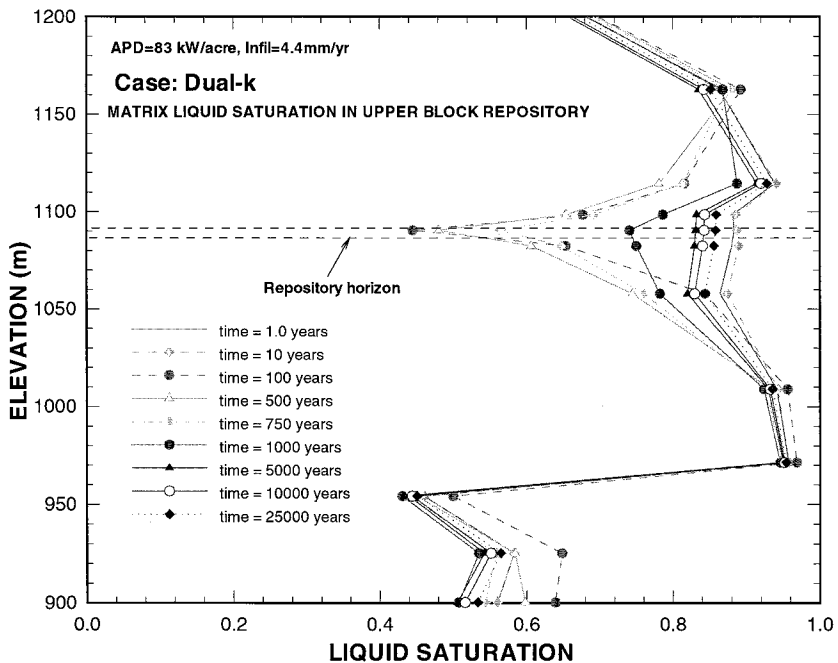


Fig. 15. Matrix vertical saturation profiles through the center of the upper repository block during thermal loading; Dual-permeability, APD = 83 kW/acre, infiltration = 4.4 mm/year.

conditions, a time dependent heat source was applied uniformly at the repository horizon for a total of 10,000 years.

Figs. 3 and 4 show the evolution of temperature. For this thermal loading and infiltration rates, boiling conditions develop in 10 years. Within the central part of the potential repository, the boiling zone extends with time, reaching a maximum of 50 m below and 150 m above the repository horizon, between 500 and 1000 years (shown in both Figs. 3 and 4). In the boiling zone convective heat transfer dominates, and the temperature remains constant at about 95°C. This boiling condition continues for about 2000 years. Complete dry-out conditions do not develop at the repository throughout the thermal loading cycle, because net liquid influx exceeds the rate of vaporization at the repository horizon. In 1000 years, temperature in the central heated area of the 2-dimensional cross-section rises to 93°C at the base of the PTn, 95°C at the repository, 75°C at the top of Calico Hills and 55°C 50 m below the water table. The computed maximum temperature at the water table is 58°C and occurs in 5000 years, long after repository temperatures have decreased (Fig. 4). Temperature conditions at the top of the model are also presented in the figures and labeled top layer of as TCw. However, temperatures within this layer are probably dominated by the surface temperature, and the specified model grid at this location does not correctly reflect temperature variations near the surface of the Mountain. Future models will consider alternative methods for treatment of the top boundary condition.

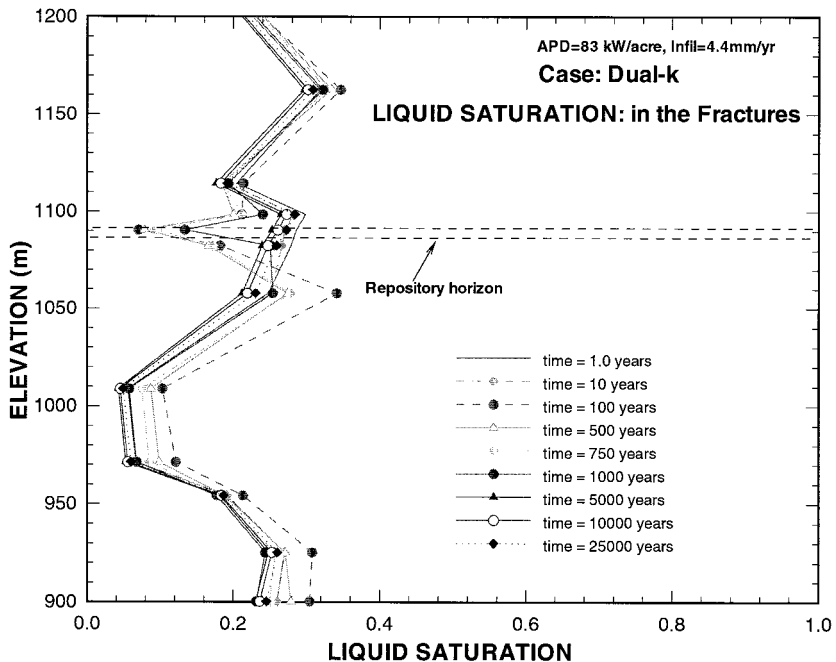


Fig. 16. Fracture vertical saturation profiles through the center of the upper repository block during thermal loading; Dual-permeability, APD = 83 kW/acre, infiltration = 4.4 mm/year.

At the repository horizon, temperatures rise to boiling conditions from 10 to 100 years and remain constant for up to 2000 years. After 2000 years the computed unsaturated zone and repository temperatures begin to decline even though local boiling still persists at the repository horizon. After 10,000 years, maximum temperature at the repository is only 72°C.

2.1.2. Saturation

During the thermal loading cycle, the saturation distributions change significantly, both spatially and temporally, near the repository. Figs. 5 and 6 show the saturation in the matrix and fracture continua at 1000 years. Repository thermal loading leads to a decrease in saturation of the matrix close to the repository and an increase in saturation in the condensation zone, 50 m above the repository. During this period the net influx of ambient water into the repository exceeds the rate of vaporization caused by heating. Under these conditions, there is a net downward flow, even through the low permeability zeolitic Calico Hills formations, throughout the thermal loading cycle. The gas flux vectors also show strong convection patterns near the repository.

To better understand the evolution of saturation and evaluate the rewetting period in the thermal loading cycle, we examine the response of a single vertical column at the center of the repository. In particular, we are interested in short and long term responses for comparison with dual-permeability modeling results.

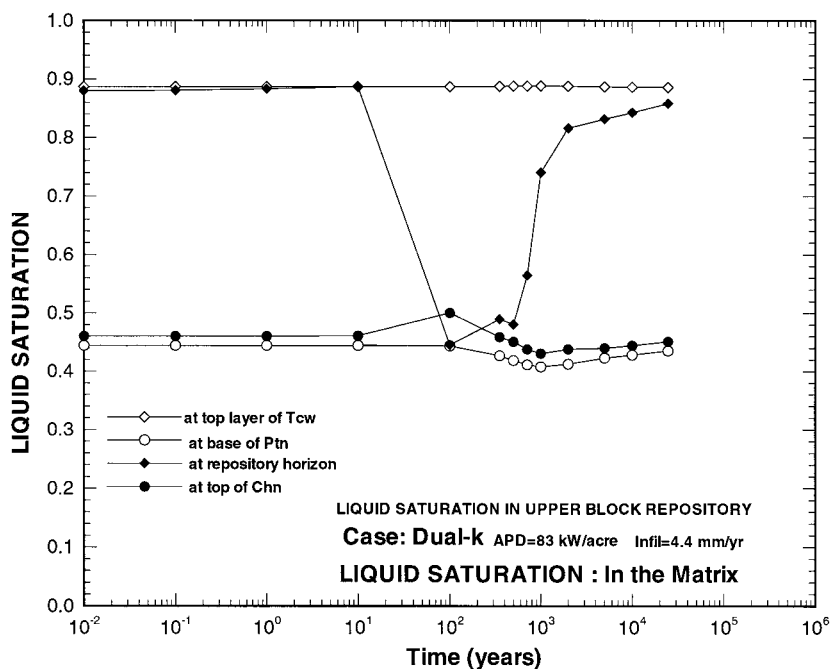


Fig. 17. Matrix liquid saturation at selected depths in the center of the upper repository block during thermal loading; Dual-permeability, APD = 83 kW/acre, infiltration = 4.4 mm/year.

For this column, the evolution of saturation in the matrix continuum over the loading cycle was investigated (Figs. 7 and 8). The saturation in the matrix is found to change significantly only in the boiling zone, within 100 m of the repository. The minimum saturation is 0.38 for the matrix continuum. This occurs within 100 years, when boiling conditions are established. Between 100 and 1000 years, although boiling continues and expands, liquid saturation within the boiling zone actually rises, because heat generation from the repository is not high enough to vaporize the liquid influx into the boiling region.

Matrix liquid saturation at the top of the CHn formation increases and reaches its maximum in 100 years (Fig. 7). The increase in saturation at the top of the CHn is mainly due to condensation of repository heat-driven vapor flux. Fig. 8 shows that maximum matrix saturation changes occur within about 100 m of the repository horizon. The matrix saturation at the southern and northern ends of the repository remain essentially unchanged throughout the thermal loading cycle and rewetting of the repository horizon occurs uniformly. At about 1000 years though the boiling area is still extensive, the average matrix liquid saturation at the repository recovers to a value of 0.85, from about 0.38 at 100 years. Further rewetting of the de-saturated area and the decay in the thermal load leads to a decline in temperature thereby halting the boiling process.

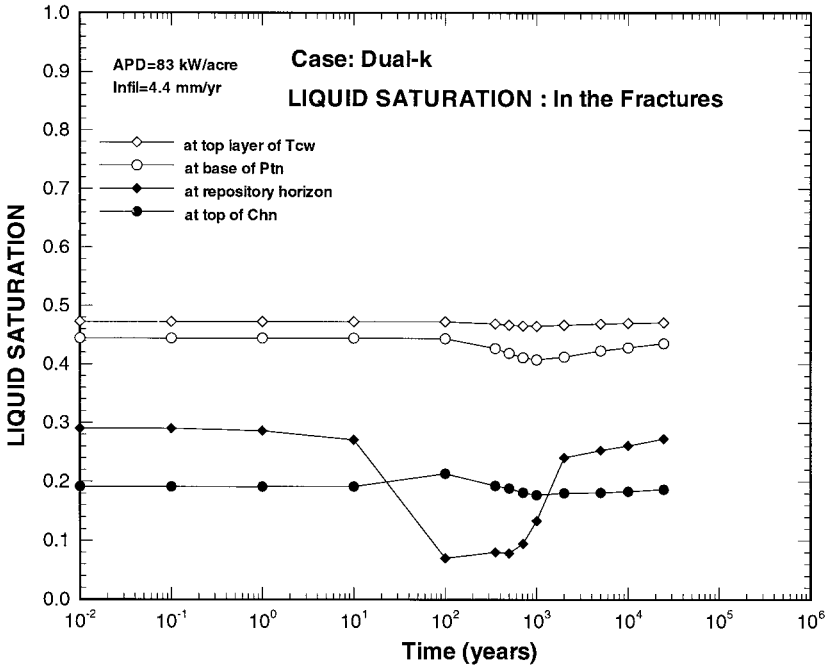


Fig. 18. Fracture liquid saturation at selected depths in the center of the upper repository block during thermal loading; Dual-permeability, APD = 83 kW/acre, infiltration = 4.4 mm/year.

2.1.3. Percolation flux

The changes in percolation flux at the repository horizon are associated closely with changes in saturation conditions, which is related to the intensity of boiling, dry-out and rewetting processes. Figs. 9 and 10 show the detailed evolution of the vertical liquid fluxes, at the top and bottom of the repository, respectively. Thermal loading leads to a large increase in the liquid flux into the repository. Note again that fluxes just above and below the repository are always towards the repository.

For the first 10 years after waste emplacement, liquid influx into the repository increases by a factor of 10 to 30 due to strong capillary suction, as compared with the net infiltration (Fig. 10). Most of the influx liquid is released from the nearby matrix or is from condensation. After 100 years the influx into the repository decreases to an average of about 10 mm/year at the bottom edge and about 60 mm/year at the top edge of the repository.

2.2. Dual-permeability simulation results with 4.4 mm/year infiltration, 2-D model

2.2.1. Temperature

As in the ECM case, the dual- k simulation uses the thermal loading scenario of an equivalent APD of 83 kW/acre. Figs. 11 and 12 show the changes in temperature

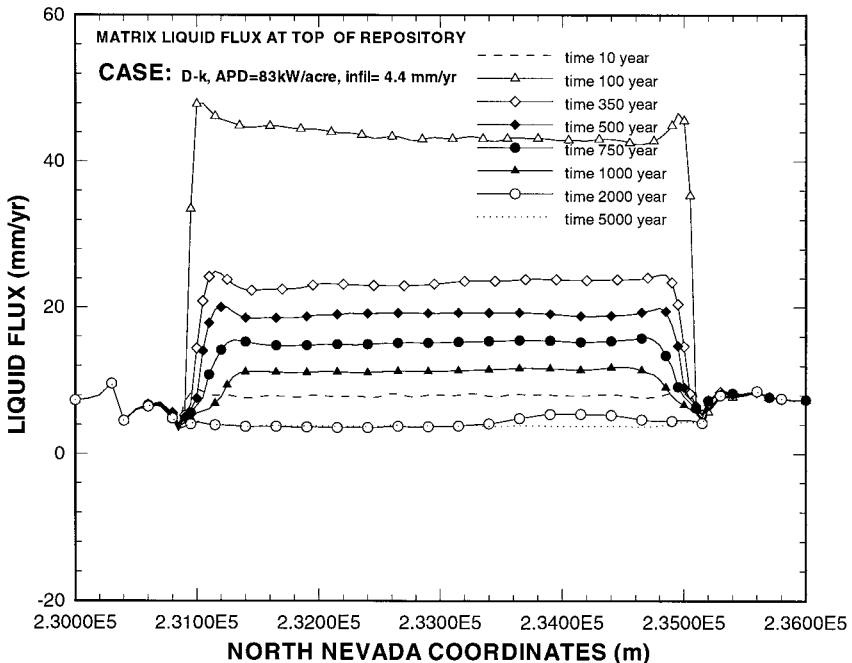


Fig. 19. Matrix liquid flux crossing the top boundary of the repository; Dual-permeability, APD = 83 kW/acre, infiltration 4.4 mm/year.

spatially and temporally for this case. Boiling conditions develop after about 100 years of thermal loading. At 500 years, the temperatures within the 100 m zone above and below the repository reaches 95°C (slightly lower boiling point temperature due to higher effective fluid mobility, and therefore, lower saturation pressure). Strong convective heat transfer occurs at or near boiling conditions. This boiling condition lasts for an additional 500 years (Figs. 11 and 12). Like in the ECM case, complete dry-out conditions do not develop at the repository throughout the thermal loading cycle.

The simulated boiling zone extends to a maximum of 100 m vertically above and below the repository horizon for 500–1000 years, as shown in Fig. 12. In this period, convective heat transfer dominates and the temperature remains constant at about 95°C in the boiling zone. For the dual-*k* model the boiling zone does not extend to the base of the PTn (unlike in the ECM case). In 1000 years, temperature at base of the PTn rises to 65°C. At this time, the repository temperature reaches 95°C, and the temperatures at the top of Calico Hills and at 50 m below the water table are at 76°C and 57°C, respectively. The computed maximum temperature at the water table is 59°C, which occurs at about 5000 years.

At the repository horizon, temperatures rise to boiling conditions in 20–100 years and remain constant (Fig. 12) until 2000 years when the computed repository temperatures begin to gradually decline. After 10,000 years, the temperature at the repository decreases to 60°C, and drops to 42°C after 25,000 years.

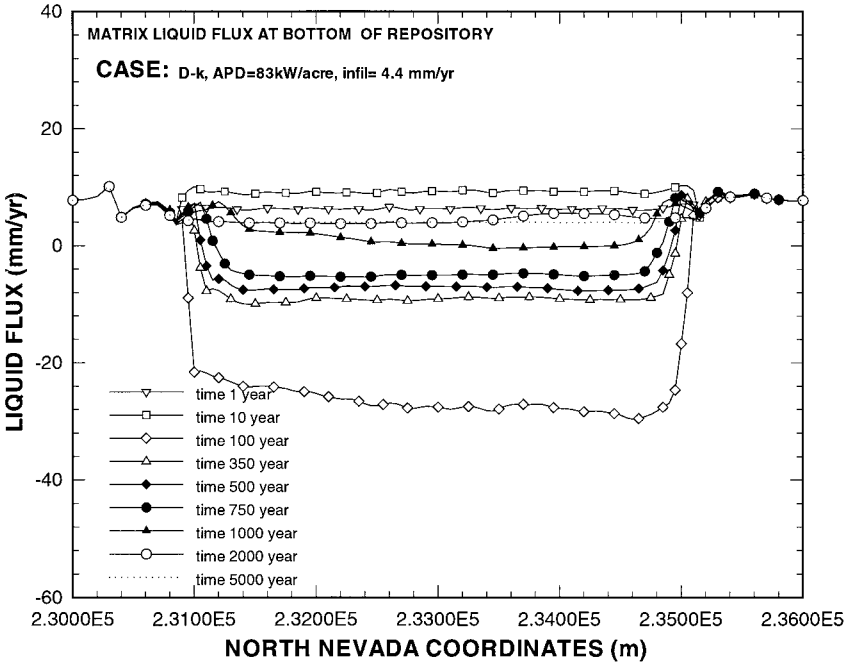


Fig. 20. Matrix liquid flux crossing the bottom boundary of the repository; Dual-permeability, APD = 83 kW/acre, infiltration 4.4 mm/year.

2.2.2. Saturation

Figs. 13 and 14 show the matrix and fracture saturation distributions after 1000 years of thermal loading. The matrix and fracture saturation at the repository is lowest at 500–1000 years. After 1000 years the matrix and fracture saturation at the repository horizon increases, while temperature remains nearly constant. As in the ECM case, not enough heat is generated to vaporize all the liquid flowing back to the repository.

The gas flux shows strong convection patterns near the repository throughout the boiling period (Fig. 14). Circulation cells develop at both the southern and northern ends of the repository. Vapor condensation zones are formed directly above the repository, below the TCw. Below the repository heat driven gas flow moves up-dip of the repository, along the top of Calico Hills to form circulation cells at the southern end of the repository.

The changes in matrix saturation along the 1-D column are shown in Fig. 15 and the fracture saturations are presented in Fig. 16. The minimum matrix liquid saturation is about 40%, and the fracture saturation is as low as 5%, at about 100 years, as soon as boiling conditions are established. As in the Effective Continuum Method case, with 4.4 mm/year infiltration complete dry-out does not occur.

A small increase in liquid saturation at the top of the Calico Hills formation is predicted in about 100 years, both in the matrix and the fracture continuum (Figs. 17 and 18). This saturation increase is mainly due to condensation of repository-driven vapor

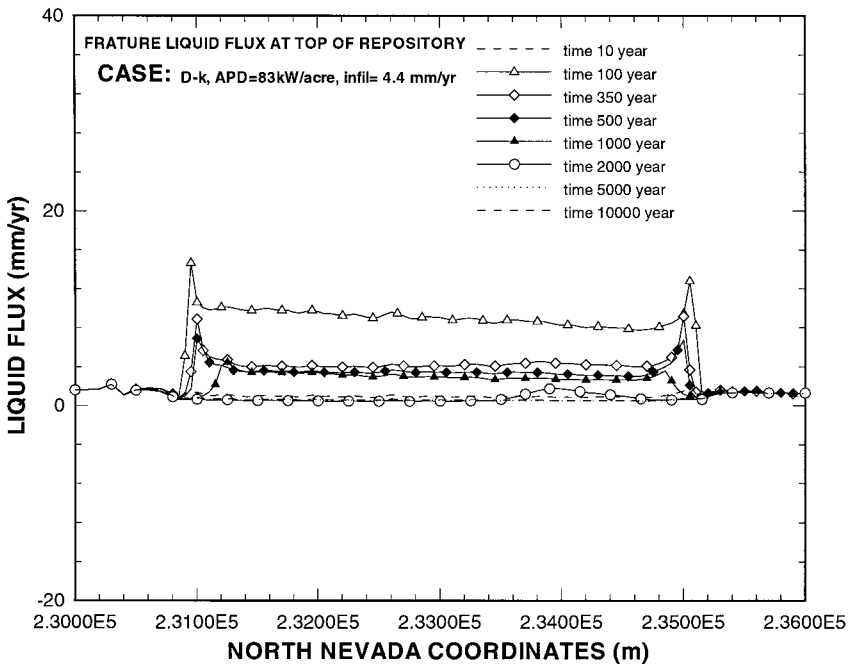


Fig. 21. Fracture liquid flux crossing the top boundary of the repository; Dual-permeability, APD = 83 kW/acre, infiltration 4.4 mm/year.

flux. The figures show that matrix saturation near the south and north ends of the repository horizon remains unchanged throughout the thermal loading cycle, and that rewetting processes are very uniform. In 1000 years of thermal loading, though the boiling zone is still extensive, average liquid saturation at the repository recovers to 75% in matrix, and to 15% in fractures. The rewetting of the fracture continuum lags significantly behind that of the matrix continuum.

2.2.3. Percolation flux

The repository percolation fluxes simulated by the dual-permeability model are shown in Figs. 19–22. Figs. 19 and 20 give the liquid influx into the repository from matrix flow. Figs. 21 and 22 show the influx from the fracture. As can be seen from the four figures, both matrix flow and fracture flow into the repository increase by as much as a factor of 10, during the thermal loading period, compared to the ambient infiltration rate of 4.4 mm/year. The flux at the top boundary of the repository is fairly uniform.

The contrast in the results of the ECM and dual-*k* approaches can be seen by comparing the results in Figs. 9 and 10 (ECM) to the results in Figs. 19–22 (dual-*k*). This numerical study predicts that at early times, 10 years, the Effective Continuum Method model has a much higher downward matrix flow into the repository, mainly due to the ‘drier’ (higher matrix suction) condition. At later times, after 100 years, the two

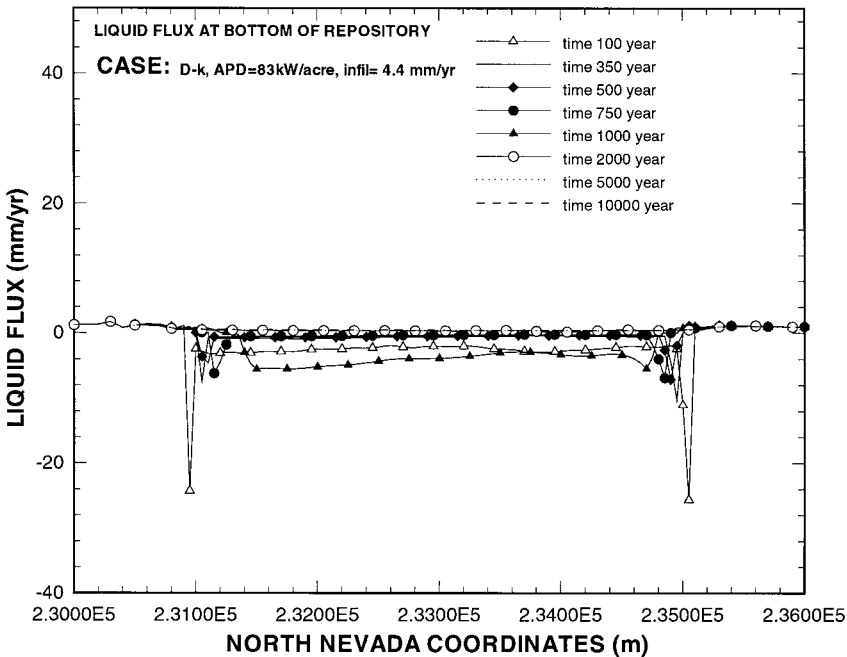


Fig. 22. Fracture liquid flux crossing the bottom boundary of the repository; Dual-permeability, APD = 83 kW/acre, infiltration 4.4 mm/year.

models give similar flux calculations. The flow crossing the bottom boundary of the repository, is very similar for the two models during the entire thermal loading period. Both the ECM and dual- k models predict enhanced liquid flux at the ends of the repository on bottom boundary due to edge cooling and condensation.

2.3. 3-D model results

In this section we present and discuss the results of our numerical simulation using the 3-D model with the base case thermal load of 87.6 kW/acre (85 MTU/acre) and variable infiltration, and using the ECM formulation.

The T–H behavior and effects of thermal loading on the moisture, gas, and heat flow within the mountain are discussed using 1-D, 2-D plots for comparison with the 2-D cross-section model results. We also present 3-D plots. For this discussion, a column at the center of the of the repository is selected to evaluate the evolution of temperature and liquid saturation.

2.3.1. Temperature and saturation changes at repository

Fig. 23 shows the temperature and saturation variations for the base case simulation scenario, for a column within the central portion of the waste emplacement block. The

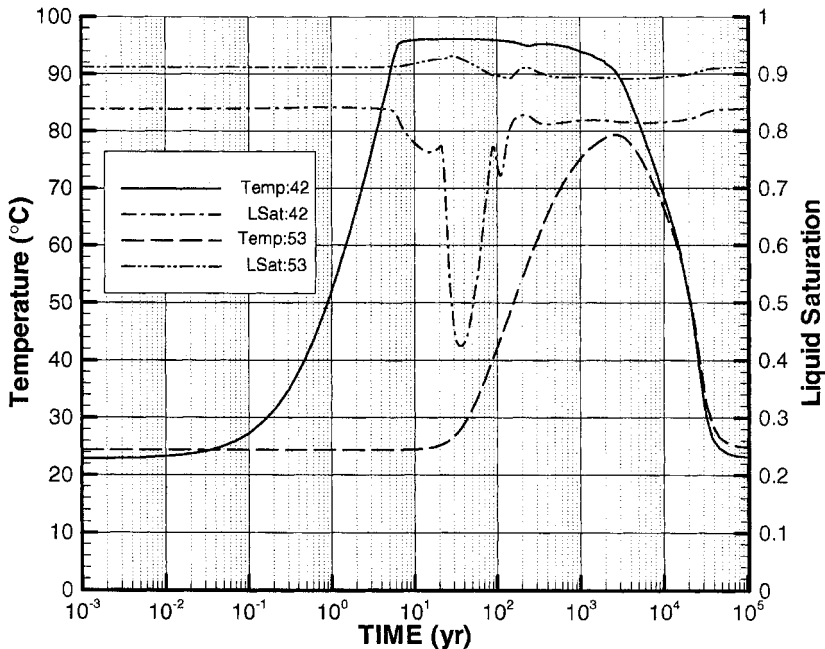


Fig. 23. Variations in temperature and saturation at the center of the repository, at Column #1, base-case infiltration and base-case thermal load scenario, 3-D simulation.

simulation results (labeled as Temp:42 on the figures), indicate that the highest temperature reached at the repository location is about 96°C, or the boiling point at the simulated pressure. The maximum temperature within the repository occurs after less than 10 years of thermal loading and continues for 1000 years.

Also shown in Fig. 23 are the temperature variations at the basal vitrophyre layer, the bottom of the TSw unit, labeled as ‘Temp:53’ on the figures. The figure shows that temperature rises up to about 80°C within the basal vitrophyre zone directly below the repository. Temperatures at the basal vitrophyre zone reach maximum values after 1000–4000 years of thermal loading.

In addition, the variations in matrix liquid saturations are shown in Fig. 23. At the repository (labeled as ‘LSat:42’) the 3-D model also predicts no complete ‘dry-out’. The driest zones at the repository have 20 to 30% liquid saturation and occur between 30 to 50 years after thermal loading is applied. The re-wetting and re-drying during the boiling period, at a time of 4–1000 years, indicate that during certain periods, water flowing back to the repository by capillary suction may be larger than that of outflow by evaporation/boiling. The figures also show that there are very small variations in saturation (labeled as ‘LSat:53’) at the basal vitrophyre from repository thermal effects. At the edge of the repository, the boiling period will generally be shorter and temperature increases lower compared to this central location.

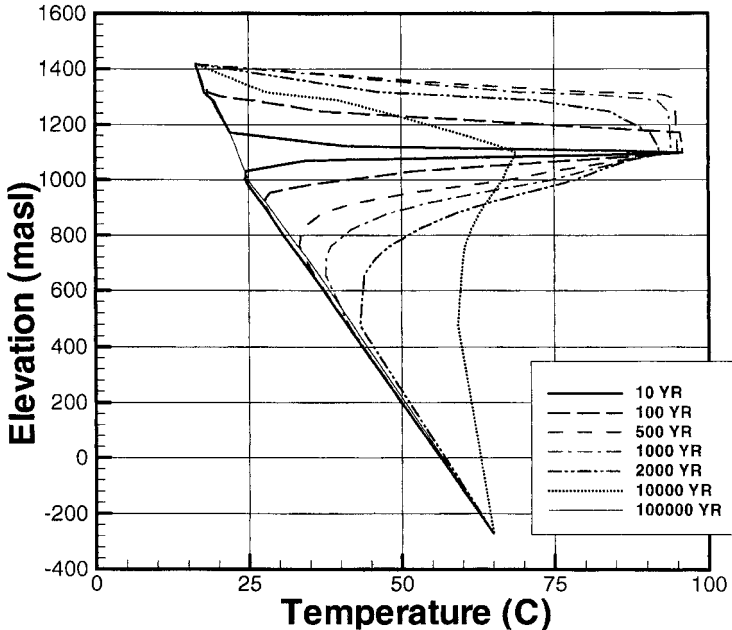


Fig. 24. Vertical temperature profiles along Column #1, at the center of the emplacement block, base-case infiltration and base-case thermal load scenario, 3-D Simulation.

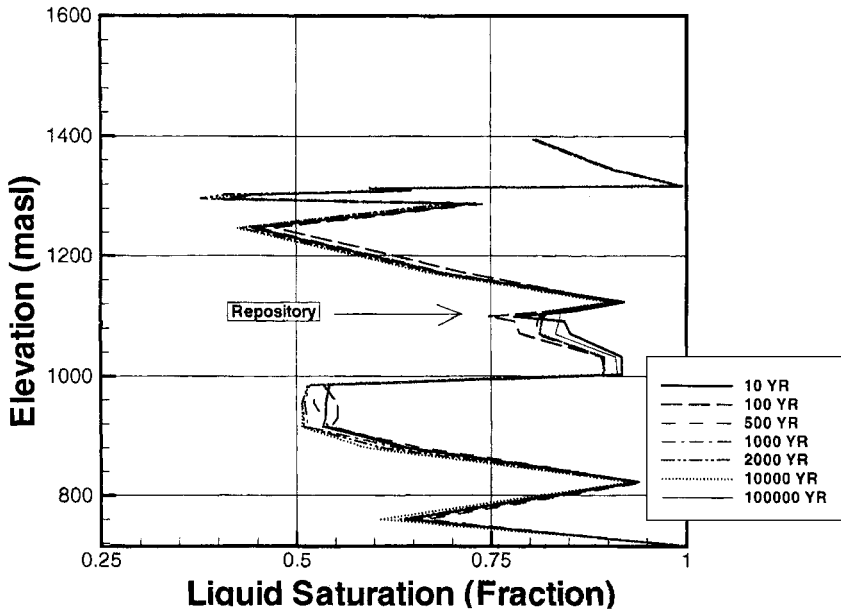


Fig. 25. Vertical saturation profiles along Column #1, at the center of the emplacement block, base-case infiltration and base-case thermal load scenario, 3-D simulation.

2.3.2. 1-D vertical spatial temperature and saturation profiles

The 1-D vertical temperature profiles, which are plotted along the same three vertical columns are presented and discussed in this section for the base case. Fig. 24 gives the

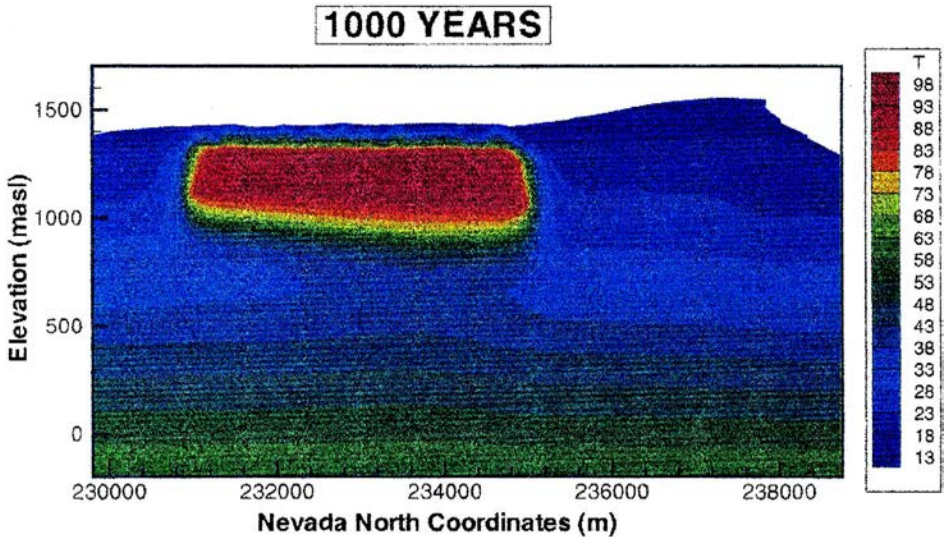


Fig. 26. Vertical temperature profiles of 1000 years along south–north (S–N) cross-section, base-case infiltration and base-case thermal load scenario, 3-D simulation.

results for Column #1, at the center of the repository block. It can be seen that the hottest spot is always on the repository horizon. The temperature at the repository horizon increases to the maximum of about 96°C. This boiling zone vertically expands upwards from the repository level, up to 200 m thick between 100 and 1000 years of thermal loading. During this period, ‘heat pipe’ phenomena are observed. The temperature values at which a heat pipe occurs corresponds to the boiling point under the ambient condition of moisture and atmospheric pressure.

After 1000 years, the temperature gradually decreases at the repository, and eventually returns to near ambient condition after 10,000 years. Fig. 24 also shows that there is significant increase in temperature at the water table at an elevation of 730 m, reaching its peak value at about 10,000 years of waste emplacement.

Examination of the 3-D modeling results indicates that these boiling zones does not extend into the PTn units for all the infiltration and thermal load scenarios considered (the ECM 2-D model predicts it extends into the PTn).

The saturation profiles along Column #1 are given in Fig. 25. The figure shows, in general, that large high-liquid-saturated, condensate zones are not formed above or

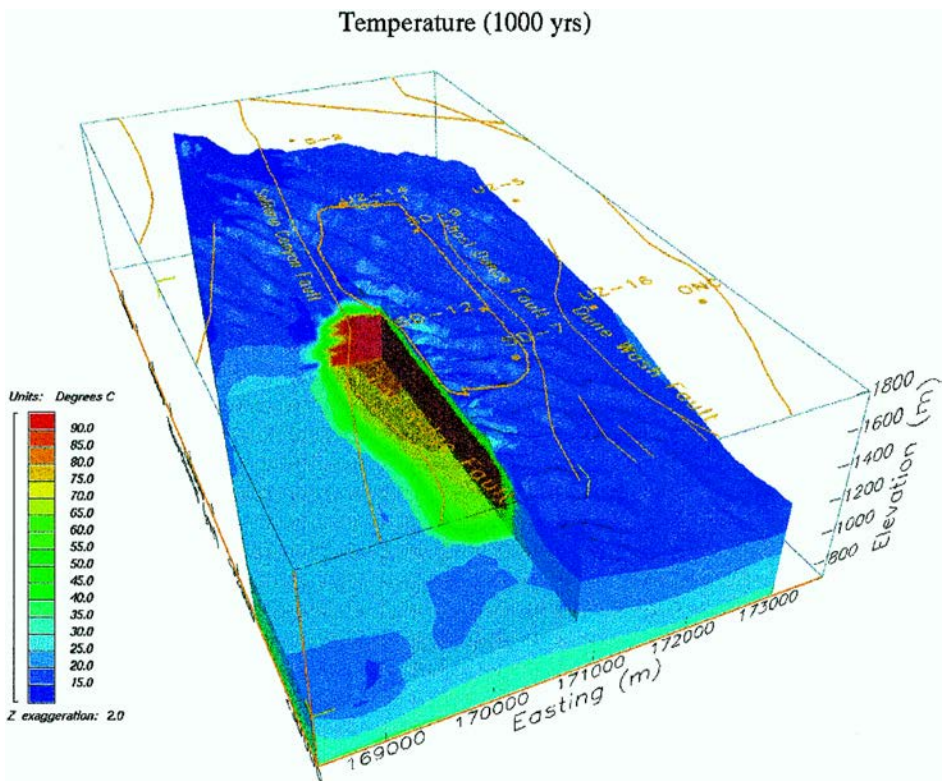


Fig. 27. 3-D perspective view of temperature profiles of 1000 years, base-case infiltration and base-case thermal load scenario.

below the repository during the entire thermal loading period. Significant ‘dry-out’ at the repository level may occur for higher thermal loads and low infiltration rates or when small matrix blocks are used to represent average conditions at the repository (explicit drift model). The condensation zones above the repository have very small increases in liquid saturations, with peak values between 10 and 100 years.

2.3.3. 2-D and 3-D temperature and saturation profiles

The spatial temperature variations and distributions can be easily seen using 2-D vertical cross-sections or 3-D plots. Fig. 26 shows vertical temperature profiles along the south–north (S–N) cross-section at 1000 years. After 1000 years of thermal loading the boiling zone is predicted to extend up to 200 m in the vertical direction. Lateral change in the region affected by boiling conditions is small. This indicates that vertical heat transfer is the dominant mechanism during a boiling period.

The 3-D plots of temperature profiles for the base-case scenario at 1000 years are shown in Fig. 27. The figure shows that a boiling zone exists at the repository level. This boiling zone which starts less than 10 years after thermal loading reaches maximum extent in about 100 years, within the central part of the repository which remains at boiling conditions for over 1000 years.

2.3.4. Effects of thermal loading on vertical moisture flow

The effect of thermal loading on vertical moisture flow above and below the repository level are discussed using the 3-D simulation results.

Fig. 28 shows the simulated vertical fluxes of water along Column #1 at the center of the repository. In these figures, a positive value for water or heat fluxes means downward flow, and a negative value denotes upward flow. We select only three times

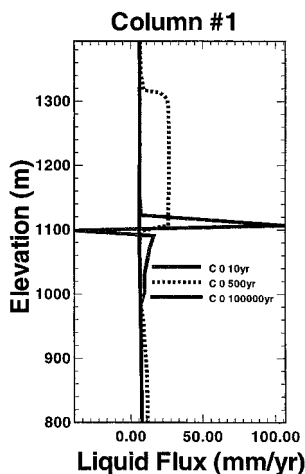


Fig. 28. Vertical water flow along Column #1, at the center of the repository block, base-case infiltration and base-case thermal load scenario, 3-D simulation.

—10, 500 and 10,000 years—in the plot because there are significant differences in the modeled fluxes mainly for these times. The highest back-flow to the repository (at an elevation of 1100 m) occurs at 10 years. Within this column, the water back flow from above the repository exceeds 100 mm/year. Below the repository the maximum is about 40 mm/year. After 500 years, the back flow is much smaller and only from above the repository. After 10,000 years, the repository flow returns to the ambient conditions.

Figs. 29 and 30 show a map view of the vertical liquid flux in the model layer immediately above the repository at 100 and 1000 years after waste emplacement. The period 100 years after waste emplacement shows the greatest downward liquid flux above the repository, with a maximum of between 140 and 180 mm/year, as shown in Fig. 29. Small, isolated areas of upward liquid flow are observed around the ends of the

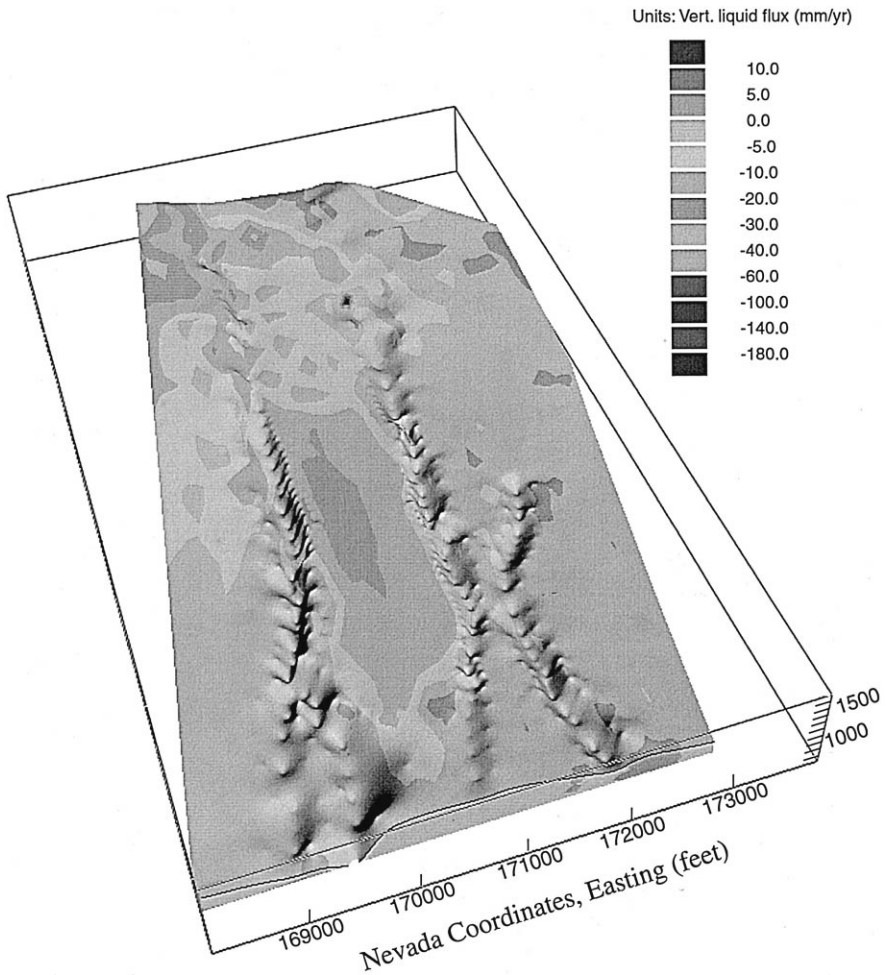


Fig. 29. Vertical liquid phase flux immediately above the repository after 100 years, base-case infiltration and base-case thermal load scenario, 3-D simulation.

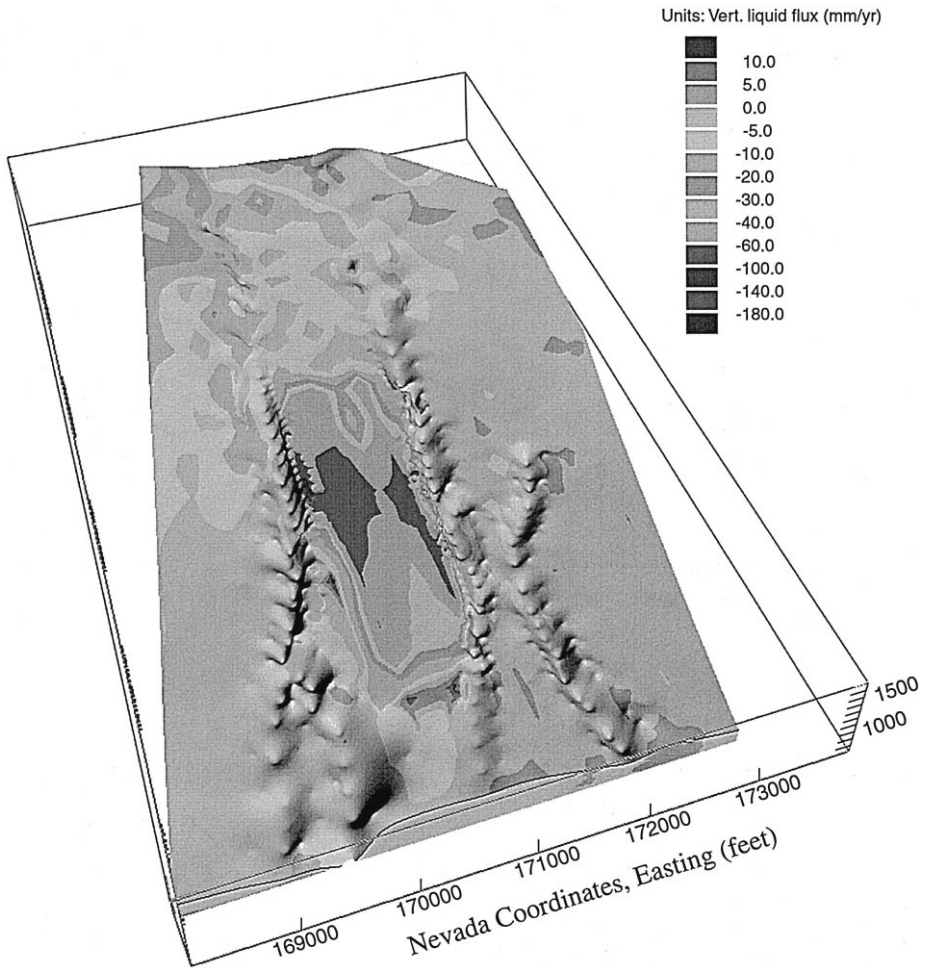


Fig. 30. Vertical liquid phase flux immediately above the repository after 1000 years, base-case infiltration and base-case thermal load scenario, 3-D simulation.

repository. At 1000 years, the maximum downward liquid flux is reduced to less than 30 mm/year, as shown in Fig. 30.

2.3.5. Temperature distribution at the water table

As the repository produces heat, first the unsaturated zone will heat up, and then as the heat pulse spreads, it will contact the water table and begin heating the saturated zone. The water table is approximately 300 m below the repository, so a significant temperature rise is not observed at the water table until 1000 years after waste emplacement. For base case thermal loading/infiltration scenario, the temperature at the water table under the central portion of the repository, rises only about 10°C in 1000 years. Fig. 31 shows a map of the temperature at the water table after 10,000 years of

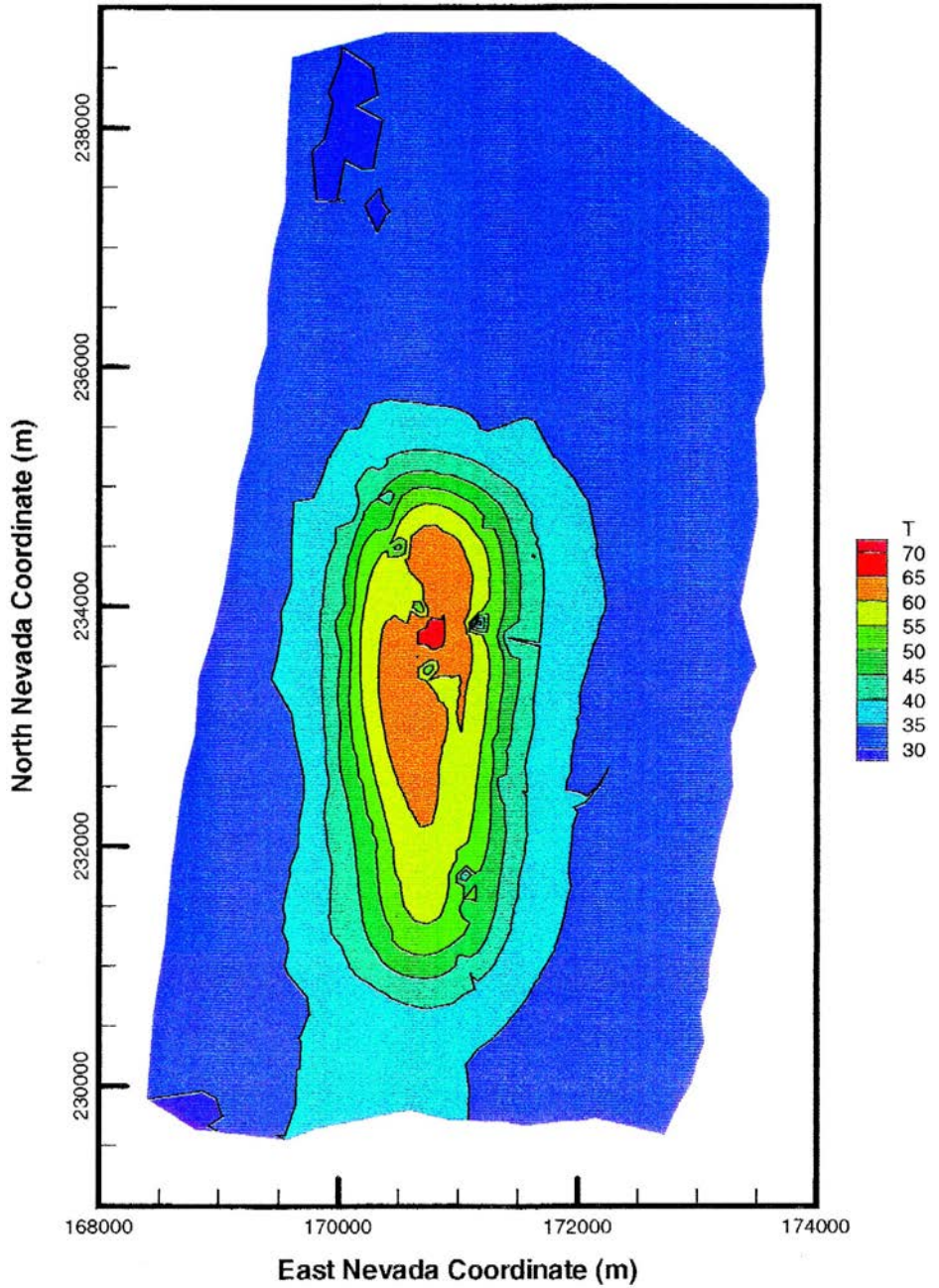


Fig. 31. Temperature at the water table after 10,000 years, base-case infiltration and base-case thermal load scenario, 3-D simulation.

thermal loading. The maximum water table temperature, is about 35°C above the pre-emplacement temperature. The highest temperatures are reached under the northern portion of the repository. Temperatures under the southern portion of the repository are lower because the thermal conductivity of the unaltered rock under the southern portion of the repository is lower than that of the altered rock under the northern portion of the repository. The repository is also closer to the water table in the north.

3. Conclusions

A systematic modeling study of effect of thermal loading on the moisture, gas and heat flow in the unsaturated zone of Yucca Mountain has been carried out. The study is based on a 2-D north–south vertical cross-section, using both the ECM and the dual- k and a 3-D ECM numerical models. Both the 2-D and 3-D models allow the temperature at the water table to vary by moving the UZ model bottom boundary fixed temperature condition to at least 500 m below the water table. This treatment of the model bottom boundary condition allows us to investigate the effects of the thermal load on the water table thermal conditions. The study uses a baseline simplified model that neglects, the effects of thermal hydrological chemical (THC) and thermal hydrological mechanical (THM) coupling as well as flow channeling effects on the evolution of the flow fields. Future studies can build on such a baseline model by considering the effects the effects of chemical deposition, changes in stress-field or flow channeling on effective permeability under thermal loading conditions

The numerical models predict about a 30–35°C temperature increase at the water table. This indicates that the model with a fixed temperature boundary applied at the water table, may overestimate the rate of cooling of the repository. Placement of the bottom temperature boundary condition does not affect the maximum temperature it water table. This is because such treatment only affects the cool down phase (> 1000 years) of the thermal loading cycle. It does not influence heating phase (0–1000 years).

Thermal loading at the repository results in significant changes in the moisture and temperature distributions at the repository horizon and the zone directly above and below it. Strong liquid and gas flow fields, which are several orders of magnitude above ambient conditions, develop near the repository. With the thermal loading scenario used, for the 2-D model with 4.4 mm/year infiltration, the maximum temperature at the repository is about 95°C (the numerical grid is not fine enough to resolve higher temperatures expected near the waste canister). The average temperature of the boiling zone is about 95°C. This boiling zone is confined to the TSw hydrogeological unit. The 3-D model also predicts repository horizon temperatures of 95–97°C.

At the top of the CHn (vitric/zeolitic interface), predicted temperature rises to about 70–75°C after about 2000 years. The predicted near surface temperatures (top of the TCw) are probably dominated by the top temperature condition and may not correctly model near surface temperature conditions.

The boiling and rewetting processes at the repository are controlled by the available heat and liquid flow at the repository horizon. Using the 2-D model with an infiltration rate of 4.4 mm/year of and a thermal load of 83 MTU/acre, and the rock properties

used in the TSw hydrogeological unit, heat pipe conditions develop above and below the repository in 10–100 years. This enhances heat transfer from the repository to the water table and to the top boundary. At this infiltration rate, no complete dry-out zone is predicted. Analysis of the flux pattern at the top and bottom boundaries of the repository shows that the liquid always flows into the repository throughout the thermal loading cycle. The 3-D model with spatially varying infiltration rate and slightly higher average thermal load indicates complete dry-out is possible particularly in areas of low infiltration. Flux at the top and bottom boundaries is always towards the repository. In the central part of the repository percolation flux (back flow) reaches 100 mm/year in the low infiltration areas due to high capillary pressure gradients. The dual- k models show that the flow is predominantly through the fracture continuum.

This study also shows that for a 4.4 mm/year infiltration rate, the ECM and dual- k modeling approaches provide similar simulation results, in terms of temperature and moisture flow and distributions. The only difference is that at early times, the ECM model predicts more extensive boiling conditions than does the dual- k model. The 2-D model represents fairly well the changes in thermal-hydrological conditions along the N–S cross-section predicted by the 3-D model.

Acknowledgements

The authors are grateful to R.M. Zimmerman, and C. Oldenburg, R. Ahlers, N. Francis, D. Bryan and D. Mangold, for the critical and careful review of this report. Thanks are due to Maryann Villavert and Colleen Haraden, for the help in preparing the manuscript. This work was supported by the Director, Office of Civilian Radioactive Waste Management, US Department of Energy, through Memorandum Purchase Order EA9013MC5X between TRW Environmental Safety Systems and the Ernest Orlando Lawrence Berkeley National Laboratory (Berkeley Lab). The support is provided to Berkeley Lab through the US Department of Energy Contract No. DE-AC03-76SF00098.

References

- Ahlers, C.F., Bandurraga, T.M., Bodvarsson, G.S., Chen, G., Finsterle, S., Wu, Y.S., 1995a. Summary of model calibration and sensitivity studies using the LBNL/USGS. Three-Dimensional Unsaturated Zone Site-Scale Model, Yucca Mountain Site Characterization Project Report, September.
- Ahlers, C.F., Bodvarsson, T.M.b.G.S., Chen, G., Finsterle, S., Wu, Y.S., 1995b. Performance analysis of the LBNL/USGS three-dimensional unsaturated zone site-scale model. Yucca Mountain Project Milestone 3GLM105M, Lawrence Berkeley National Laboratory, Berkeley, CA.
- Ahlers, C.F., Shan, C., Haukwa, C., Cohen, A.B.J., Bodvarsson, G.S., 1996. Calibration and prediction of pneumatic response of at Yucca Mountain, Nevada using the unsaturated zone flow model. Yucca Mountain Project Milestone OB12M.
- Bandurraga, T.M., 1996. Geological model development and vertical layering scheme for the numerical grid. In: Bodvarsson, G.S., Bandurraga, M. (Eds.), Development and Calibration of the Three-dimensional Site-scale Unsaturated-zone Model of Yucca Mountain, Nevada, Chap. 2. Yucca Mountain Site Characterization Project Report, Lawrence Berkeley National Laboratory, Berkeley, CA.

- Bodvarsson, G.S., Bandurraga, T.M. (Eds.), 1996. Development and Calibration Of The Three-Dimensional Site-Scale Unsaturated-Zone Model Of Yucca Mountain, Nevada. Yucca Mountain Site Characterization Project Milestone OBO2, LBNL Report 39315, Lawrence Berkeley National Laboratory, Berkeley, CA.
- Braithwaite, J.W., Nimick, F.B., 1984. Effect of host-rock dissolution and precipitation on permeability in a nuclear waste repository in tuff. Rep. SAN84-0192, Sandia National Laboratory, Albuquerque, NM, September.
- Buscheck, T.A., Nitao, J.J., 1991. Modeling hydrothermal flow in variably saturated, fractured, welded tuff of the Yucca Mountain project. Proceedings of the 5th Workshop Flow and Transport through Unsaturated Fractured Rock. Tucson, AZ.
- Buscheck, T.A., Nitao, J.J., 1992. The impact of thermal loading on repository performance at Yucca Mountain. Proceedings 3rd International High Level Radioactive Waste Management Conference, Las Vegas, NV, April 12–16.
- Buscheck, T.A., Nitao, J.J., 1993a. Repository-heat-driven hydrothermal flow at Yucca Mountain: Part I. Modeling and analysis. *Nucl. Technol.* 104 (3), 418–448.
- Buscheck, T.A., Nitao, J.J., 1993b. The analysis of repository-heat-driven hydrothermal flow at Yucca Mountain. Proceedings, 4th International High Level Radioactive Waste Management Conference. Las Vegas, NV, April 26–30.
- Buscheck, T.A., Nitao, J.J., 1993c. The impact of repository-heat-driven hydrothermal flow on hydrological performance at Yucca Mountain. Proceedings, 4th International High-Level Radioactive Waste Management Conference. Las Vegas, NV, April. Also, UCRL-JC-112333, Lawrence National Laboratory, Livermore, CA.
- Buscheck, T.A., Nitao, J.J., 1993d. Repository-heat-driven hydrothermal flow at Yucca Mountain: Part I. Modeling and analysis. *Nucl. Technol.* 104 (3), 449–471.
- Buscheck, T.A., Nitao, J.J., 1993e. Repository-heat-driven hydrothermal flow at Yucca Mountain: Part II. Large-scale in situ heater tests. *Nucl. Technol.* 104 (3), 418–448.
- Buscheck, T.A., Nitao, J.J., 1994. The importance of thermal loading conditions to waste package performance at Yucca Mountain. Proceedings, XVIII International Symposium on the Scientific Basis for Nuclear Waste Management. Kyoto, Japan, October 23–27, 1994.
- Buscheck, T.A., Nitao, J.J., Saterlie, S.F., 1994. Evaluation of thermo-hydrological performance in support of the thermal loading systems study. Proceedings, International High Level Radioactive Waste Management Conference. Las Vegas, NV, May 22–26.
- Flint, A.L., Hevesi, J.A., Flint, L.E., 1996. Conceptual And Numerical Model Of Infiltration For The Yucca Mountain Area, Nevada. U.S. Geological Survey Water Resources Investigation Report, U.S. Geological Survey, Denver, CO.
- Francis, N.D., 1997. The base case Thermal properties for TSPA-VA modeling. Memo distribution. Sandia National Laboratories, Albuquerque, NM, April 16.
- Francis, N.D., Mishra, S., Ho, C.K., Arnold, B.W., Bandurraga, M., Wu, Y., Statham, W.H., Zhang, H., 1996. Thermal-hydrologic Modeling of the Potential Repository at Yucca Mountain Using a 3-D Site-Scale Unsaturated-Zone Model. Yucca Mountain Site Characterization Project Milestone T6533, W.B.S. #1.2.5.4.3, WA-211.
- Haukwa, C., Wu, Y.S., Bodvarsson, G.S., 1996. Thermal loading studies using the unsaturated zone model. In: Bodvarsson, G.S., Bandurraga, M. (Eds.), Development and Calibration Of The Three-Dimensional Site-Scale Unsaturated-Zone Model of Yucca Mountain, Nevada, Chap. 13. Yucca Mountain Site Characterization Project Milestone OBO2, Lawrence Berkeley National Laboratory, Berkeley, CA.
- M and O, Recommended layoff concepts report, BCAA00000-01717-00001, Rev 00, Civilian Radioactive Waste Management System Management and Operating Contractor, Las Vegas, NV, July.
- M and O CRWMS, 1995. FY 95 CDA Update waste Stream Follow on Data, CRWMS M and O interoffice Correspondence, VA.SA.JD. 04/95.046, April 7.
- Mondy, L.A., Wilson, R.K., Bixler, N.E., 1983. Comparison of waste emplacement configurations for a nuclear waste repository in tuff, IV, thermohydrological analysis. Rep. SAND83-0757, Sandia National Laboratory, Albuquerque, NM, Aug.
- Nielsen, D.R., van Genuchten, M.Th., Biggar, J.W., 1986. Water flow and solute transport in the unsaturated zone. *Water Resour. Res.* 22 (9), 89S–108S.
- Nitao, J.J., 1988. Numerical modeling of the thermal and hydrological environment around a nuclear waste

- package using the equivalent continuum approximation: Horizontal emplacement. Rep. UCID-21444, Lawrence Livermore National Laboratory, Livermore, CA.
- Nitao, J.J., 1989. V-TOUGH, An Enhanced Version of the TOUGH Code for the Thermal and Hydrologic Simulation of Large-Scale Problems in Nuclear Waste Isolation. Rep. UCID-21954, Lawrence Livermore National Laboratory.
- Nitao, J.J., Buscheck, T.A., Chesnut, D.A., 1992. The implications of episodic non-equilibrium fracture-matrix flow on site suitability and total system performance. Proceedings, 3rd International High Level Radioactive Waste Management Conference. Las Vegas, NV, April 26–30.
- Ogniewicz, Y., Tien, C.L., 1979. Porous heat pipe, Heat Transfer Thermal Control and Heat Pipes. In: Olstad, W.B. (Ed.), *Progress in Astronautics and Aeronautics*. Martin Summerfield Ser., Vol. 70. AIAA, Washington, DC.
- Pruess, K., 1987. TOUGH user's guide. Nuclear Regulatory Commission Report NUREG/CR-4645; Also Rep. LBL-20700, Lawrence Berkeley Laboratory, Berkeley, CA.
- Pruess, K., 1991. TOUGH2—A general purpose numerical simulator for multiphase fluid and heat flow. Rep. LBL-29400, Lawrence Berkeley Laboratory, Berkeley, CA, May.
- Pruess, K., Narasimham, T.N., 1991. A practical method for modeling fluid and heat flow in fractured porous media. *Soc. Pet. Eng. J.* 25 (1), 14–26.
- Pruess, K., Tsang, Y.W., 1993. Modeling of strongly heat-driven flow processes at a potential high-level nuclear waste repository at Yucca Mountain, Nevada. Proceedings, 4th International High Level Radioactive Waste Management Conference. Las Vegas, NV, April 26–30.
- Pruess, K., Tsang, Y.W., 1994. Thermal modeling for a potential high-level nuclear waste repository at Yucca Mountain, Nevada. Rep. LBL-35381 UC-600, Lawrence Berkeley Laboratory, Berkeley, CA, March.
- Pruess, K., Wang, J.S.Y., 1984. TOUGH—A numerical model for nonisothermal unsaturated flow to study waste canister heating effects. In: McVay, G.L. (Ed.), *Scientific Basis for Nuclear Waste Management*, Vol. 26. Mater. Res. Soc. Symp. Proc. Elsevier, NY, pp. 1031–1038.
- Pruess, K., Wang, J.S.Y., Tsang, Y.W., 1990a. On thermohydrologic conditions near high-level nuclear wastes emplaced in partially saturated fractured tuff: Part I. Simulation studies with explicit consideration of fracture effects. *Water Resour. Res.* 26 (6), 1235–1248.
- Pruess, K., Wang, J.S.Y., Tsang, Y.W., 1990b. On the thermohydrologic conditions near high-level nuclear wastes emplaced in partially saturated fractured tuff: Part 2. Effective continuum approximation. *Water Resour. Res.* 26 (6), 1249–1261.
- Ramspott, L.D., 1991. The constructive use of heat in an unsaturated tuff repository. Proceedings, 2nd International High Level Radioactive Waste Management Conference, Las Vegas, NV, April 28–May 2.
- Ruffner, D., Johnson, G.L., Platt, E.A., Blink, J.A., Doering, T., 1993. Drift emplaced waste package thermal ecrepsins. American Nuclear Society, Proceedings 4th International High-Level Radioactive Waste Management Conference, Las Vegas, NV, April.
- Ryder, E.E., 1992. Results of two-dimensional near-field thermal calculations in support of M and O study on repository thermal loading.
- Sass, J.H., Lachenbruch, A.H., Dudley Jr., W.W., Priest, S.S., Munroe, R.J., 1988. Temperature, Thermal Conductivity And Heat Flow Near Yucca Mountain, Nevada Some Tectonic And Hydrologic Implications. U.S. Geological Survey report USGS-OFR-87-649; DE89 002697, U.S. Geological Survey.
- St. John, C.M., 1985. Thermal analysis of spent fuel disposal in vertical emplacement, boreholes in a welded tuff repository. Rep. SAND84-7207, Sandia National Laboratory, Albuquerque, NM, Nov., 1985.
- Travis, B.J., Nuttall, H.E., 1987. Two-dimensional numerical simulation of geochemical transport in Yucca Mountain. Rep. LA10532-MS, Los Alamos National Laboratory, Los Alamos, NM, Dec., 1987.
- Travis, B.J., Hodson, S.W., Nuttall, H.E., Cook, T.L., Rundberg, R.S., 1984. Numerical Simulation of Flow and Transport in Fractured Tuff, Vol. 26. Mater. Res. Soc. Symp. Proc. Elsevier, NY, pp. 1039–1047.
- TRW, 1996. Thermal loading study for FY 1995. Report B000000000-01717-5705-00016, January 31, 1996.
- Tsang, Y.W., Pruess, K., 1987. A study of thermally induced convection near a high-level nuclear waste repository in partially saturated fractured tuff. *Water Resour. Res.* 23 (10), 1958–1966.
- Udell, K.S., 1985. Heat transfer in porous media considering phase change and capillarity—the heat pipe effect. *Int. J. Heat Mass Transfer* 28 (2), 485–495.
- Warren, J.E., Root, P.J., 1963. The behavior of naturally fractured reservoirs. *Soc. Pet. Eng. J., Trans. AIME* 228, 245–255.

- Wittwer, C., Chen, G., Bodvarsson, G.S., Chornack, M., Flint, A., Kwicklis, E., Spengler, R., 1994. The development of the LBL/USGS three-dimensional site-scale model of Yucca Mountain, Nevada. Research Report, Lawrence Berkeley Laboratory, Berkeley, CA.
- Wittwer, C., Chen, G., Bodvarsson, G.S., Chornack, M., Flint, A., Kwicklis, E., Spengler, R., 1995. Preliminary development of the LBL/USGS three-dimensional site-scale model of Yucca Mountain, Nevada. Research Report LBL-37356, UC-814, Lawrence Berkeley National Laboratory, Berkeley, CA.
- Wu, Y.S., Pruess, K., 1988. A multiple-porosity method for simulation of naturally fractured petroleum reservoirs. *SPE Reservoir Eng.* 3, 327–336.
- Wu, Y.S., Chen, G., Bodvarsson, G., 1995. Preliminary Analysis Of Effects Of Thermal Loading On Gas And Heat Flow Within The Framework Of The LBNL/USGS Site-Scale Model. Report LBL-37729 UC-814, N/A, N/A, Lawrence Berkeley National Laboratory, Berkeley, CA.
- Zimmerman, R.M., 1983. First phase of small diameter heater experiments in tuff. Proceedings, 27th U.S. Symposium on Rock Mechanics, Texas A&M University, College Station, TX, June, 1983.
- Zimmerman, R.M., Blanford, M.L., 1986. Expected thermal and hydrothermal environments for waste emplacement holes based on G-tunnel heater experiments. Proceedings, 27th U.S. Symposium on Rock Mechanics, pp. 874–882.
- Zimmerman, R.M., Nimick, F.B., Board, M.B., 1995. Geo-engineering Characterization of Welded Tuffs from Laboratory and Field Investigations, Vol. 44. Mater. Res. Soc. Symp. Proc. Materials Research Society, Pittsburgh, PA, pp. 547–554.